UNCLASSIFIED
CONFIDENTIAL

Copy 6
RM L55F17

NACA RM L55F17

3 1176 00007 7876

NACA

RESEARCH MEMORANDUM

STATIC LONGITUDINAL AND LATERAL STABILITY AND CONTROL CHARACTERISTICS OF AN AIRPLANE CONFIGURATION HAVING A WING OF TRAPEZOIDAL PLAN FORM WITH VARIOUS TAIL AIRFOIL SECTIONS AND TAIL ARRANGEMENTS AT A MACH NUMBER OF 6.86

By Jim A. Penland, David E. Fetterman, Jr., and Herbert W. Ridyard

Langley Aeronautical Laboratory
Langley Field, Va.

CLASSIFICATION CHANGED
UNCLASSIFIED
To
By authority of TIB #35 Date 9/16/60

CLASSIFIED DOCUMENT

This material contains information affecting the National Defense of the United States within the meaning of the espionage laws, Title 18, U.S.C., Secs. 793 and 794, the transmission or revelation of which in any manner to an unauthorized person is prohibited by law.

NATIONAL ADVISORY COMMITTEE FOR AERONAUTICS

WASHINGTON

August 15, 1955

CONFIDENTIAL
UNCLASSIFIED

NATIONAL ADVISORY COMMITTEE FOR AERONAUTICS

RESEARCH MEMORANDUM

STATIC LONGITUDINAL AND LATERAL STABILITY AND CONTROL CHARACTERISTICS OF AN AIRPLANE CONFIGURATION HAVING A WING OF TRAPEZOIDAL PLAN FORM WITH VARIOUS TAIL AIRFOIL SECTIONS AND TAIL ARRANGEMENTS AT A MACH NUMBER OF 6.86

By Jim A. Penland, David E. Fetterman, Jr., and Herbert W. Ridyard

SUMMARY

An investigation has been carried out in the Langley 11-inch hypersonic tunnel to determine the static longitudinal and lateral stability and control characteristics of an airplane configuration having a trapezoidal wing with a modified hexagonal airfoil section and equipped with various tail airfoil sections and tail arrangements. Tail airfoil sections tested were a 10° wedge, a flat-plate section, and a series of composite airfoils consisting of flat plates forward of the hinge lines and wedges behind the hinge lines. The tests were made at a Mach number of 6.86 and a Reynolds number of 343,000 based on the wing mean aerodynamic chord. Data were obtained for angles of sideslip up to 10° and angles of attack up to 25° for the complete model with the cruciform 10° wedge horizontal and vertical tails and for the complete model with various tail arrangements.

INTRODUCTION

Previous experimental investigations at the Langley Laboratory of the supersonic airplane configuration shown in figure 1 have been made by using wedge airfoil sections for the horizontal and vertical tails. These investigations have supplied the longitudinal and lateral stability and control characteristics for a complete model and various combinations of its components at Mach numbers of 4.06 and 6.86 (refs. 1 to 6).

The purpose of the present investigation was to determine the effect of tail airfoil sections on the stability and control characteristics of the aircraft configuration tested in references 1 to 6. A series of tail airfoil sections were tested which simulated an airfoil whose section could be changed from a flat plate to a section consisting of a flat plate forward of the hinge line and a wedge behind the hinge line. Such airfoils would provide a tail configuration in which the airfoil sections could be changed during a flight of changing Mach number to provide the variable effectiveness necessary. Tail arrangements, other than the original cruciform horizontal- and vertical-tail configuration and those reported in references 5 and 6 were tested to provide additional comparisons of some of the many possible arrangements.

The design of the basic configuration (fig. 1) incorporated relatively large leading-edge radii on both the wing and tail surfaces in order to provide adequate heat capacity at the leading edge to keep the heat-transfer rates, at hypersonic speeds, within feasible limits. From recent information on the beneficial effects of leading-edge sweep and the use of materials capable of withstanding higher temperatures, it appears that smaller radii could have been used with resulting improvement in the aerodynamic characteristics. However, in order to provide a consistent basis of comparison, the large leading-edge radii were also used for the present tests.

Six-component data have been obtained for the complete model with the various tail arrangements and tail airfoil sections. The present paper contains the static longitudinal and lateral stability and control results for various horizontal-tail deflections.

COEFFICIENTS AND SYMBOLS

The results of the tests are presented as coefficients of forces and moments. The longitudinal data are referred to the stability-axis system and the lateral data are referred to the body-axis system. The body- and stability-axis systems are illustrated in figure 2 and the axis-transfer equations are given in the appendix. As indicated in the appendix, lateral-force and pitching-moment coefficients are unchanged in this transfer of axes. The moment reference is at 54 percent of the wing mean aerodynamic chord (52.66 percent of the body length measured from the nose). The coefficients and symbols are defined as follows:

C_L lift coefficient, $-Z_S/qS$

C_D drag coefficient, $-X_S/qS$ (at $\beta = 0^\circ$)

C_{D_o} minimum drag coefficient

[redacted]

L/D	lift-drag ratio, C_L/C_D
C_N	normal-force coefficient, $-Z_B/qS$
C_Y	lateral-force coefficient, Y/qS
C_l	rolling-moment coefficient, L_B/qSb
C_m	pitching-moment coefficient, $M'/qS\bar{c}$
C_n	yawing-moment coefficient, N_B/qSb
X	force along X-axis
Y	force along Y-axis
Z	force along Z-axis
L	moment about X-axis
M'	moment about Y-axis
N	moment about Z-axis
q	free-stream dynamic pressure
S	total wing area including area submerged in fuselage
b	wing span
c	wing chord
$\bar{c}$	wing mean aerodynamic chord
M	Mach number
R	Reynolds number
α	angle of attack, deg
β	angle of sideslip, deg
i_H	incidence angle of horizontal tail, deg

[redacted]

C_{m_α} rate of change of pitching-moment coefficient with angle of attack, $\left(\frac{\partial C_m}{\partial \alpha}\right)_{\alpha=0}$, per deg

C_{Y_β} rate of change of lateral-force coefficient with angle of sideslip at zero sideslip angle, $\left(\frac{\partial C_Y}{\partial \beta}\right)_{\beta=0}$, per deg

C_{l_β} rate of change of rolling-moment coefficient with angle of sideslip at zero sideslip angle, $\left(\frac{\partial C_l}{\partial \beta}\right)_{\beta=0}$, per deg

C_{n_β} rate of change of yawing-moment coefficient with angle of sideslip at zero sideslip angle, $\left(\frac{\partial C_n}{\partial \beta}\right)_{\beta=0}$, per deg

Subscripts:

B body-axis system

S stability-axis system

MODELS AND APPARATUS

Models

The basic model used for the present tests is shown in figure 1. Details of this model are given in the three-view drawing (fig. 3) and in the table of geometric characteristics (table I). The model was equipped with removable tail surfaces which enabled the testing of tail surfaces with the following airfoil sections: 10° wedge (the results of which were previously presented in refs. 1, 2, and 5), flat plate, and composite sections made up of flat plates extending from the leading edge to the hinge line, with 10°, 20°, and 30° total-angle wedges extending from the hinge line to the trailing edge (ref. 7). All tail airfoil sections had approximately identical leading-edge radii (fig. 4).

The previous tests of references 2 and 5 have shown the bottom vertical tail to be most effective in producing lateral stability at high angles of attack; however, from take-off and landing considerations, a tail surface in this location is undesirable. Therefore, in order to retain some of the directional stability of the lower vertical tail and to eliminate, to a large extent, its take-off and landing disadvantages,

a stub of the lower vertical-tail configuration was tested (figs. 4 and 5). The addition of a lower stub tail, having an exposed area of one-quarter of the exposed, bottom vertical-tail area, to the conventional top vertical and horizontal tails was believed sufficient to give positive values of the lateral-stability parameter C_{n_β}, throughout the angle-of-attack range tested. Sketches of the stub tail and the various tail airfoil sections tested are shown in figure 4.

In addition, the model with 10° wedge tail airfoil sections was tested with the tail surfaces rotated 45° from the original vertical and horizontal positions. Designations for the various tail configurations tested are shown in figure 5.

The complete model (equipped with the 10° wedge tail airfoil sections) mounted for testing in the tunnel is shown in figure 6. A discussion of some of the design features of the model is included in reference 1.

Balance and Model Support

Six-component force and moment measurements were made by means of two strain-gage balances. Five components, including normal force, lateral force, pitching moment, rolling moment, and yawing moment, were measured on a balance mounted inside the model. The sixth component, chord force, was obtained on a two-component external balance measuring normal force and chord force. In addition, a one-component external balance was used to measure pitching moment in some of the pitch tests.

The five-component balance was initially designed to measure only four components; therefore, in order to adapt the balance for use in the present program, strain gages were added to the balance sting and calibrated to measure rolling moment. This method of obtaining a rolling-moment component resulted in less sensitivity than desired.

The model was attached to the balance so that constant geometry between model and balance was maintained for all test angles. The model was placed at an angle of sideslip by means of a bent sting; angles of attack were obtained by rotating the model and balance about a horizontal axis normal to the wind stream. This type of model rotation necessitated a correction to the static angles of attack and sideslip and these corrections combined with the model deflections due to aerodynamic loads were incorporated in computing the corrected test angles. Model deflections were obtained through the use of angles measured from schlieren photographs and the balance-deflection calibration.

Wind Tunnel

The tests were conducted in the Langley 11-inch hypersonic tunnel. For this investigation, the tunnel was equipped with a single-step two-dimensional nozzle constructed of Invar. The nozzle was designed by the method of characteristics with a correction made for boundary layer and operates at an average Mach number of 6.86. The duration of each run was about 80 seconds, and the variation of test-section Mach number with time is negligible after the first 15 seconds of running time. This constant Mach number flow made it possible to obtain forces for several angles of attack during each run. The model was held at low angles of attack for starting and stopping the runs in order to minimize shock loads on the strain-gage balance which supports the model.

Tests

Tests were made at an average stagnation temperature of 675° F to avoid air liquefaction (ref. 8), a stagnation pressure of 20 atmospheres absolute, and a test Mach number of 6.86. These conditions correspond to a Reynolds number of 343,000 based on wing mean aerodynamic chord. The absolute humidity was kept to less than 1.87×10^{-5} pounds of water per pound of dry air for all tests. Tests were made at angles of sideslip from -5° to 10° through an angle-of-attack range of -5° to 25°. The model was tested with horizontal-tail incidences of 0°, about -10°, and -20°.

PRECISION OF DATA

The probable uncertainties in the force and moment coefficients for individual tests points — due to the balance system and variations in the dynamic pressure — have been evaluated and are presented as follows:

C_L	±0.03
C_{D_o}	±0.006
C_N	±0.02
C_m	±0.005
C_Y	±0.005
C_n	±0.0015
C_l	±0.003

In general, the faired curves should be more accurate than these values.

The angle of attack α and angle of sideslip β were accurate within ±0.10°.

[redacted]

RESULTS

The experimental aerodynamic characteristics of the model with various tail airfoil sections and tail-surface locations are given in tables II to IV. Plots representing portions of the data included in these tables are presented in figures 7 to 19.

The variations of C_L, C_D, and L/D with angle of attack for the model at $\beta = 0^\circ$ with the different tail airfoil sections at $i_H = 0^\circ$ are shown in figure 7. Figure 8 presents similar data for the model with the X-tail configuration having a 10° wedge tail section. In figure 9, the variations of C_m with α for the complete model at $\beta = 0^\circ$ with the various tail airfoil sections at $i_H = 0^\circ$, $i_H \approx -10^\circ$, and $i_H = -20^\circ$ are presented. In order to show the effect of the wing on the pitching-moment characteristics of the model, data for the body-tail configuration are also included in figure 9.

The effects of tail airfoil section on the variations of the longitudinal characteristics C_L, C_D, L/D, and C_m with angle of attack for the model at $\beta = 0^\circ$ are presented in figures 10 to 13. Some of these data are taken from figures 7 and 9 and are repeated here for comparison purposes. The erratic characteristics in the pitching-moment variations of the model in the angle-of-attack range 0° to 10° with $i_H \approx -10^\circ$ (see fig. 9 or fig. 13(c)) are due partly to the effect of the wing wake on the horizontal tail which, as can be seen in the three-view drawing (fig. 3), is directly in line with the wing.

The effects of tail airfoil section on the variations of the lateral characteristics C_Y, C_l, and C_n with sideslip angle of the model at $\alpha = 0^\circ$ are shown in figure 14.

Figure 15 presents the variations of the minimum drag coefficient and the static stability derivatives C_{m_α}, C_{Y_β}, C_{l_β}, and C_{n_β} with angle of tail flare for the complete model. Values of these parameters obtained with the 10° wedge tail airfoil section are also included for comparison purposes.

The results of changing the tail-surface geometry (stub-tail configuration) and location (X-tail configuration) both having 10° wedge airfoil sections are given in figures 16 to 19. The variations of C_Y, C_l, and C_n with sideslip angle for the stub-tail configuration at various angles of attack are shown in figure 16. The pitching-moment characteristics at $\beta = 0^\circ$ of the complete model, X-tail configuration, and stub-tail configuration are presented in figure 17, and the lateral

stability characteristics at $\alpha = 0^\circ$ for these configurations are presented in figure 18.

The variations of the lateral-stability derivatives C_{Y_β}, C_{l_β}, and C_{n_β} with angle of attack for the stub-tail and other tail configurations previously reported are given in figure 19. Data for all tail configurations shown, except the stub tail, were obtained from references 2 and 5. From the variations of C_{n_β} with angle of attack, it is apparent that at the higher angles of attack, the stub tail, having only 25 percent of the original exposed lower tail area, gave about 33 percent of the effectiveness obtained previously from the original lower, vertical fin. The effectiveness of the stub tail does not vary directly with its area because it is operating in a region of high dynamic pressure brought about by the compression wave emanating from the nose of the fuselage, particularly at high angles of attack.

Typical schlieren photographs of the complete model equipped with the tail airfoil sections tested are shown in figure 20; and figure 21 contains schlieren photographs of the model with various tail arrangements using a 10° wedge tail airfoil section.

Langley Aeronautical Laboratory,
National Advisory Committee for Aeronautics,
Langley Field, Va., June 9, 1955.

[redacted]

APPENDIX

AXIS-TRANSFER EQUATIONS

The equations for transfer of force and moment coefficients from the body-axis system to the stability-axis system are as follows:

$$C_{Y_S} = C_{Y_B}$$

$$C_{l_S} = C_{l_B} \cos \alpha + C_{n_B} \sin \alpha$$

$$C_{n_S} = C_{n_B} \cos \alpha - C_{l_B} \sin \alpha$$

$$C_{m_S} = C_{m_B}$$

$$C_{L_S} = C_{N_B} \cos \alpha - C_{D_B} \sin \alpha$$

$$C_{D_S} = C_{D_B} \cos \alpha + C_{N_B} \sin \alpha$$

[redacted]

REFERENCES

1. Penland, Jim A., Ridyard, Herbert W., and Fetterman, David E., Jr.: Lift, Drag, and Static Longitudinal Stability Data From an Exploratory Investigation at a Mach Number of 6.86 of an Airplane Configuration Having a Wing of Trapezoidal Plan Form. NACA RM L54I03b, 1955.

2. Ridyard, Herbert W., Fetterman, David E., Jr., and Penland, Jim A.: Static Lateral Stability Data From an Exploratory Investigation at a Mach Number of 6.86 of an Airplane Configuration Having a Wing of Trapezoidal Plan Form. NACA RM L55A21a, 1955.

3. Dunning, Robert W., and Ulmann, Edward F.: Static Longitudinal and Lateral Stability Data From an Exploratory Investigation at Mach Number 4.06 of an Airplane Configuration Having a Wing of Trapezoidal Plan Form. NACA RM L55A21, 1955.

4. Dunning, Robert W., and Ulmann, Edward F.: Exploratory Investigation at Mach Number 4.06 of an Airplane Configuration Having a Wing of Trapezoidal Plan Form – Longitudinal and Lateral Control Characteristics. NACA RM L55B28, 1955.

5. Fetterman, David E., Jr., Penland, Jim A., and Ridyard, Herbert W.: Static Longitudinal and Lateral Stability and Control Data From an Exploratory Investigation at a Mach Number of 6.86 of an Airplane Configuration Having a Wing of Trapezoidal Plan Form. NACA RM L55C04, 1955.

6. Dunning, Robert W., and Ulmann, Edward F.: Exploratory Investigation at Mach Number 4.06 of an Airplane Configuration Having a Wing of Trapezoidal Plan Form – Effects of Various Tail Arrangements on Wing-On and Wing-Off Static Longitudinal and Lateral Stability Characteristics. NACA RM L55D08, 1955.

7. McLellan, Charles H.: A Method of Increasing the Effectiveness of Stabilizing Surfaces at High Supersonic Mach Numbers. NACA RM L54F21, 1954.

8. McLellan, Charles H., and Williams, Thomas W.: Liquefaction of Air in the Langley 11-Inch Hypersonic Tunnel. NACA TN 3302, 1954.

[redacted]

TABLE I.- GEOMETRIC CHARACTERISTICS OF MODEL

Wing:	
Area (including area submerged in fuselage), sq in.	6.24
Span, in.	4.33
Mean aerodynamic chord, in.	1.716
Root chord at plane of symmetry, in.	2.53
Tip chord, in.	0.354
Airfoil section	Hexagonal with round leading edge
Taper ratio	0.140
Aspect ratio	3.00
Sweep of leading edge, deg	38.83
Sweep of quarter-chord line, deg	29
Incidence at fuselage center line, deg	0
Dihedral, deg	0
Geometric twist, deg	0
Horizontal or vertical tails:	
Area (including area submerged in fuselage), sq in.	2.06
Span, in.	2.69
Mean aerodynamic chord, in.	0.853
Root chord at plane of symmetry, in.	1.214
Tip chord, in.	0.317
Airfoil section	Variable
Taper ratio	0.261
Aspect ratio	3.52
Sweep of leading edge, deg	22.63
Fuselage:	
Length, in.	7.50
Maximum diameter, in.	0.790
Fineness ratio	9.50
Base diameter, in.	0.790
Distance from nose to moment reference	3.950
Ogive nose length, in.	2.29
Ogive radius, in.	6.85

[redacted]

TABLE II.- AERODYNAMIC CHARACTERISTICS OF THE MODELS AT M = 6.86; R = 343,000;

FIVE-COMPONENT BODY-AXIS DATA

(a) Complete model

i_{T_1}, deg.	α_1, deg.	β_1, deg.	C_N	C_m	C_l	C_n	C_Y	i_{T_2}, deg.	α_2, deg.	β_2, deg.	C_N	C_m	C_l	C_n	C_Y
10° wedge tails															
0	- 0.02	0	0.0027	-0.0002	0.0008	0.0002	0.0007	-20	0.05	0	-0.0075	0.0180	0.0007	0.0001	-0.0014
0	.94	0	.0065	- .0047	.0007	.0003	.0000	-20	1.08	0	.0025	.0234	- .0001	.0000	- .0020
0	1.90	0	.0105	- .0088	.0005	.0002	- .0009	-20	2.27	0	.0125	.0312	- .0009	.0000	.0000
0	2.83	0	.0593	- .0114	.0012	.0000	- .0018	-20	3.10	0	.0150	.0306	- .0009	.0000	- .0007
0	3.88	0	.0751	- .0134	.0011	.0001	- .0015	-20	4.27	0	.0201	.0705	- .0001	.0002	- .0016
0	5.93	0	.1168	- .0206	- .0002	.0002	- .0023	-20	6.07	0	.0753	.0924	- .0010	.0001	- .0017
0	7.87	0	.1633	- .0312	.0001	.0002	- .0024	-20	7.95	0	.1200	.0442	- .0017	.0001	- .0019
0	9.85	0	.2135	- .0394	.0018	.0003	- .0028	-20	10.00	0	.1626	.0480	.0001	.0002	- .0018
0	14.75	0	.3679	- .0754	.0026	.0002	- .0038	-20	15.10	0	.2950	.0526	- .0010	.0003	- .0026
0	19.75	0	.5735	- .1311	.0033	- .0008	- .0032	-20	20.18	0	.4597	.0475	- .0007	.0002	- .0037
0	24.58	0	.7657	- .2021	.0066	- .0011	- .0066	-20	25.27	0	.6911	.0294	.0017	.0000	- .0059
-10	0.00	0	- .0049	.0145	.0007	.0000	- .0005	0	- .13	-1.99	- .0019	.0018	- .0034	- .0013	.0154
-10	1.07	0	.0062	.0170	- .0001	- .0002	.0005	0	.00	.01	- .0013	- .0005	- .0001	.0005	.0001
-10	2.05	0	.0198	.0182	- .0010	.0002	.0002	0	.00	.99	.0024	- .0010	- .0005	.0013	- .0094
-10	3.02	0	.0354	.0222	- .0021	- .0002	- .0002	0	.03	1.98	.0038	.0016	- .0018	.0022	- .0178
-10	4.08	0	.0506	.0231	- .0022	- .0001	- .0021	0	.08	2.96	- .0003	.0012	- .0016	.0042	- .0214
-10	6.07	0	.0910	.0129	- .0035	.0000	- .0022	0	.35	3.95	.0041	- .0020	.0024	.0055	- .0395
-10	7.90	0	.1352	.0083	.0011	.0001	- .0022	0	.00	4.94	- .0024	- .0016	.0008	.0071	- .0450
-10	9.98	0	.1783	.0063	.0302	.0001	- .0021	0	.30	5.93	.0003	- .0017	.0020	.0085	- .0593
-10	15.00	0	.3224	- .0056	- .0011	- .0002	- .0037	0	.33	7.90	.0064	- .0020	.0003	.0113	- .0769
-10	19.90	0	.5043	.0010	- .0003	- .0059		0	.41	9.87	- .0001	- .0025	- .0008	.0151	- .0981
							- .0079								
Flat-plate tails															
0	- 5.17	- .01	-0.0669	0.0043	0.0005	0.0005	-0.0013	-10	9.92	0	0.1763	0.0140	-0.0021	-0.0004	0.0034
0	- 2.17	- .01	- .0342	.0031	.0028	.0006	- .0002	-10	14.75	0	.3084	.0073	- .0011	- .0004	.0051
0	- .08	- .01	- .0003	.0006	.0019	.0005	.0003	-10	19.58	0	.4797	- .0103	- .0039	- .0002	.0063
0	1.92	- .01	.0342	- .0018	.0020	.0005	.0002	-10	24.58	0	.6924	- .0424	- .0018	- .0001	.0084
0	3.75	- .01	.0709	- .0042	.0022	.0005	.0006	0	0	-5.00	.0003	- .0001	.0005	- .0015	.0397
0	5.92	- .01	.1086	- .0056	.0014	.0005	.0003	0	0	-3.92	.0038	- .0001	.0000	- .0014	.0318
0	7.75	- .01	.1719	- .0123	.0023	.0005	.0005	0	0	-2.83	.0037	- .0001	- .0003	- .0010	.0242
0	9.67	- .01	.1997	- .0171	.0013	.0006	.0001	0	0	-1.75	.0037	.0000	- .0006	- .0004	.0165
0	14.58	- .02	.3424	- .0383	- .0001	.0009	- .0001	0	0	- .58	.0037	.0000	- .0009	- .0003	.0088
0	19.58	- .01	.5262	- .0864	- .0018	.0008	.0010	0	0	.17	.0072	- .0005	.0045	- .0003	.0028
0	24.67	- .01	.7692	- .1306	- .0041	.0006	.0028	0	0	1.33	.0073	- .0005	.0043	- .0002	- .0040
-10	- 4.67	0	- .2015	.0371	.0038	- .0001	.0000	0	0	2.26	.0073	- .0005	.0041	- .0003	- .0101
-10	.27	0	- .0039	.0122	.0012	- .0004	.0017	0	0	3.18	.0067	- .0005	- .0001	.0002	- .0183
-10	2.00	0	.0252	.0156	.0002	- .0003	.0020	0	0	3.93	.0070	- .0005	.0016	.0002	- .0261
-10	3.83	0	.0500	.0184	.0004	- .0003	.0026	0	0	5.93	.0070	- .0004	.0011	.0012	- .0422
-10	5.92	0	.0918	.0139	.0006	- .0004	.0033	0	0	8.01	.0070	- .0004	.0006	.0017	- .0583
-10	7.83	0	.1342	.0231	.0000	- .0004	.0032								
20° Flared tails															
0	- 5.08	0	-0.0844	0.0108	0.0008	0.0003	-0.0004	0	0	5.58	0.0064	0.0002	-0.0003	0.0041	-0.0183
0	- 2.00	0	- .0327	.0060	.0010	.0003	.0005	0	0	7.75	.0067	.0006	- .0019	.0058	- .0697
0	- .17	0	.0021	.0000	.0020	.0005	.0006	0	0	9.75	.0072	.0004	- .0054	.0081	- .0961
0	1.83	0	.0375	- .0043	.0003	.0003	.0013	-10.4	9.92	0	.1818	.0122	- .0010	.0005	.0024
0	3.67	0	.0726	- .0074	.0014	.0002	.0020	-10.4	14.75	0	.3140	.0018	- .0020	.0006	.0029
0	5.67	0	.1093	- .0130	- .0002	.0003	.0018	-10.4	19.92	0	.4920	- .0196	- .0027	.0009	.0033
0	7.67	0	.1531	- .0205	.0003	.0002	.0024	-10.4	24.83	0	.7063	- .0572	- .0037	.0012	.0049
0	9.67	0	.2007	- .0278	- .0008	.0002	.0017	-10.4	- 4.67	0	- .1053	.0553	.0000	.0010	- .0018
0	14.50	0	.3432	- .0566	- .0024	.0003	.0019	-10.4	- 1.92	0	- .0440	.0288	.0021	.0008	- .0004
0	19.42	0	.5291	- .1053	- .0022	.0007	.0027	-10.4	0	0	- .0040	.0154	.0013	.0005	.0001
0	24.08	0	.7570	- .1684	- .0075	.0022	.0029	-10.4	1.92	0	.0250	.0183	.0012	.0006	.0006
0	0	-5.00	.0084	- .0002	.0018	- .0033	.0401	-10.4	3.83	0	.0572	.0226	- .0005	.0006	.0006
0	0	-2.08	.0085	- .0004	.0012	- .0008	.0210	-10.4	5.83	0	.0965	.0148	.0006	.0006	.0011
0	0	-1.25	.0086	.0000	.0008	- .0004	.0062	-10.4	7.75	0	.1377	.0117	- .0008	.0006	.0016
0	0	- .25	.0087	.0005	.0006	.0000	.0012	-10.4	9.83	0	.1810	.0217	- .0020	.0005	.0012
0	0	.75	.0089	.0005	.0003	.0003	- .0056	-10.4	14.58	0	.3146	.0023	- .0020	.0006	.0019
0	0	1.75	.0088	.0004	.0001	.0007	- .0128	-10.4	19.75	0	.4912	- .0201	- .0037	.0010	.0033
0	0	2.83	.0077	.0004	- .0003	.0018	- .0223	-10.4	24.75	0	.7066	- .0567	- .0055	.0014	.0055
0	0	3.67	.0063	.0003	.0003	.0027	- .0310								
20° Flared tails															
0	- 4.83	0	-0.0869	0.0184	0.0002	-0.0034	-0.0014	0	0	2.58	0.0092	-0.0012	-0.0021	0.0041	-0.0253
0	- 2.00	0	- .0320	.0092	.0033	- .0001	- .0005	0	0	3.67	.0092	- .0013	- .0024	.0056	- .0350
0	- .22	0	.0051	.0000	.0003	.0000	.0001	0	0	5.58	.0090	- .0010	- .0011	.0084	- .0536
0	2.08	0	.0506	- .0105	- .0015	- .0007	- .0002	0	0	7.50	.0079	- .0022	- .0018	.0114	- .0745
0	4.00	0	.0794	- .0142	- .0006	.0001	- .0004	0	0	9.50	.0071	- .0009	- .0045	.0149	- .0977
0	5.92	0	.1181	- .0230	- .0014	.0001	.0002	-10.2	- 4.58	0	- .1185	.0700	.0008	.0001	- .0018
0	7.92	0	.1630	- .0341	- .0011	.0001	.0003	-10.2	- 1.83	0	- .0458	.0325	.0011	.0000	- .0006
0	9.83	0	.2121	- .0428	- .0022	.0003	.0005	-10.2	.08	0	- .0010	.0143	.0021	- .0001	.0002
0	14.75	0	.3622	- .0724	- .0034	.0007	.0010	-10.2	1.83	0	.0247	.0180	.0012	.0002	.0006
0	19.58	0	.5529	- .1425	- .0059	.0009	.0015	-10.2	4.00	0	.0537	.0250	.0013	.0002	.0011
0	24.33	0	.7690	- .2184	- .0095	.0021	.0024	-10.2	5.92	0	.0969	.0133	- .0003	.0001	.0010
0	0	-4.92	.0062	- .0013	- .0002	- .0009	.0155	-10.2	7.83	0	.1403	.0070	- .0001	.0002	.0008
0	0	-2.08	.0109	- .0021	- .0007	- .0022	.0207	-10.2	9.92	0	.1829	.0053	- .0021	.0003	.0014
0	0	-1.17	.0076	- .0017	- .0012	- .0021	.0092	-10.2	14.75	0	.3236	- .0091	- .0018	.0006	.0021
0	0	- .08	.0090	- .0013	- .0014	- .0001	.0006	-10.2	19.67	0	.4980	- .0394	- .0026	.0009	.0035
0	0	.75	.0092	- .0012	- .0016	.0009	- .0074	-10.2	24.58	0	.7211	- .0819	- .0044	.0015	.0042
0	0	1.67	.0091	- .0010	- .0018	.0020	- .0149								

[redacted]

TABLE II.- AERODYNAMIC CHARACTERISTICS OF THE MODELS AT M = 6.86; R = 343,000;

FIVE-COMPONENT BODY-AXIS DATA — Continued

(a) Complete model — Concluded

i_H, deg.	α, deg.	β, deg.	C_N	C_m	C_l	C_n	C_Y	i_E, deg.	α, deg.	β, deg.	C_N	C_m	C_l	C_n	C_Y
30° Flared tails															
0	- 4.83	0	-0.0924	0.0279	0.0002	0.0005	0.0011	0	0	- 4.83	0.0057	-0.0001	-0.0001	-0.0120	0.0524
0	- 1.83	0	- .0350	.0114	- .0006	.0004	.0010	0	0	- 2.17	.0068	- .0029	- .0007	- .0043	.0247
0	.25	0	.0026	.0000	- .0007	.0002	.0016	0	0	- 1.00	.0089	- .0021	- .0011	- .0023	.0104
0	2.00	0	.0431	- .0137	- .0007	.0002	.0019	0	0	.08	.0089	- .0013	- .0014	- .0003	.0009
0	3.92	0	.0838	- .0242	.0004	.0000	.0028	0	0	.83	.0103	- .0010	- .0015	.0014	- .0070
0	5.83	0	.1251	- .0367	- .0014	.0002	.0029	0	0	1.83	.0091	- .0011	- .0018	.0032	- .0168
0	7.83	0	.1715	- .0506	- .0010	.0000	.0038	0	0	2.50	.0105	- .0008	- .0020	.0063	- .0291
0	9.75	0	.2217	- .0629	- .0033	- .0002	.0037	0	0	3.58	.0105	- .0010	- .0023	.0087	- .0394
0	14.50	0	.3753	- .1147	- .0047	- .0001	.0040	0	0	5.50	.0093	- .0013	- .0030	.0129	- .0616
0	19.33	0	.5757	- .1870	- .0071	.0000	.0061	0	0	7.42	.0094	- .0002	- .0036	.0175	- .0841
0	24.08	0	.8190	- .2764	- .0117	.0003	.0075	0	0	9.83	.0086	.0000	- .0064	.0228	- .1136
X-tail configuration															
0	- 5.08	0	-0.0814	.0058	.0009	-0.0001	-0.0012	0	0	- 5.00	0.0073	-0.0020	-0.0009	0.0039	-0.0406
0	- 2.17	0	- .0277	.0004	.0011	- .0002	- .0006	0	0	- 3.08	.0074	- .0019	- .0005	.0017	- .0230
0	- .17	0	.0036	- .0004	.0011	- .0002	- .0004	0	0	- 1.08	.0073	- .0018	- .0010	.0004	- .0077
0	1.92	0	.0351	- .0013	.0011	.0000	- .0003	0	0	- .08	.0074	- .0018	- .0003	- .0002	- .0005
0	3.83	0	.0709	- .0054	.0012	.0000	.0000	0	0	.83	.0074	- .0018	- .0006	- .0008	.0066
0	5.75	0	.1080	- .0100	.0013	.0000	- .0003	0	0	1.83	.0076	- .0017	.0001	- .0014	.0140
0	7.83	0	.1492	- .0164	.0006	- .0001	- .0004	0	0	2.83	.0077	- .0017	.0008	- .0022	.0216
0	9.67	0	.1975	- .0269	.0003	.0001	- .0019	0	0	3.75	.0078	- .0016	.0015	- .0031	.0302
0	14.75	0	.3462	- .0657	- .0008	.0001	- .0007	0	0	5.67	.0074	- .0014	- .0011	- .0059	.0533
0	19.50	0	.5288	- .1069	- .0030	- .0002	.0004	0	0	7.67	.0073	- .0012	- .0015	- .0094	.0703
0	24.33	0	.7485	- .1568	- .0050	- .0022	.0120								
Stub-tail configuration															
0	- 5.00	- 1.99	-0.0959	0.0208	0.0007	-0.0004	0.0108	0	- 5.17	1.98	-0.0943	0.0204	-0.0012	0.0013	-0.0150
0	- 2.25	- 2.00	- .0420	.0160	- .0004	- .0006	.0114	0	- 2.00	1.99	- .0408	.0146	- .0024	.0012	- .0161
0	- .17	- 2.00	- .0026	.0112	- .0008	- .0001	.0092	0	- .17	2.00	- .0029	.0060	- .0025	.0008	- .0152
0	1.83	- 2.00	.0362	- .0027	.0001	- .0005	.0093	0	1.92	1.99	.0357	- .0027	- .0016	.0012	- .0169
0	4.00	- 1.99	.0743	- .0072	.0018	- .0004	.0105	0	3.83	1.99	.0726	- .0073	- .0017	.0012	- .0171
0	5.58	- 1.99	.1130	- .0130	.0007	- .0001	.0107	0	5.68	1.99	.1126	- .0121	- .0010	.0010	- .0175
0	7.68	- 1.99	.1571	- .0224	.0022	.0004	.0108	0	7.68	1.98	.1571	- .0217	- .0013	.0006	- .0184
0	9.68	- 1.98	.2082	- .0314	.0023	.0006	.0109	0	9.67	1.97	.2061	- .0309	- .0009	.0005	- .0193
0	14.59	- 1.94	.3555	- .0659	.0033	- .0004	.0141	0	14.58	1.92	.3557	- .0658	.0004	.0015	- .0232
0	19.51	- 1.87	.5516	- .1243	.0052	- .0015	.0177	0	19.51	1.87	.5482	- .1229	.0022	.0024	- .0296
0	24.51	- 1.80	.7913	- .1975	.0081	- .0024	.0205	0	24.51	1.80	.7843	- .1946	.0062	.0034	- .0344
0	- 5.00	- 1.00	- .0957	.0210	- .0004	- .0001	.0070	0	- 5.01	2.58	- .0940	.0206	.0005	.0017	- .0196
0	- 1.83	- 1.00	- .0399	.0157	- .0007	- .0001	.0060	0	- 2.01	3.00	- .0389	.0145	- .0017	.0013	- .0213
0	- .17	- 1.00	- .0028	.0067	- .0017	.0000	.0059	0	.08	3.00	- .0014	.0060	- .0009	.0014	- .0216
0	1.83	- 1.00	.0351	- .0022	.0001	.0000	.0059	0	1.92	3.00	.0366	- .0022	- .0010	.0013	- .0225
0	3.67	- 1.00	.0722	- .0068	- .0010	.0001	.0052	0	3.92	2.99	.0740	- .0058	- .0012	.0010	- .0227
0	5.67	- 1.00	.1128	- .0127	- .0003	- .0001	.0053	0	5.75	2.99	.1103	- .0108	- .0013	.0009	- .0232
0	7.67	- .99	.1582	- .0228	.0011	.0001	.0053	0	7.69	2.98	.1565	- .0216	.0000	.0006	- .0240
0	9.83	- 1.00	.2076	- .0334	.0014	.0004	.0055	0	9.84	2.96	.2056	- .0309	- .0007	.0005	- .0257
0	14.50	- .97	.3566	- .0661	.0023	.0000	.0056	0	14.52	2.90	.3511	- .0655	.0014	.0017	- .0304
0	19.42	- .94	.5485	- .1233	.0036	- .0005	.0055	0	19.69	2.81	.5438	- .1224	.0034	.0031	- .0352
0	24.33	- .90	.7671	- .1967	.0057	- .0010	.0058	0	24.44	2.70	.7797	- .1920	.0071	.0047	- .0424
0	- 5.08	0	- .0938	.0204	- .0006	.0003	.0024	0	- 5.09	3.97	- .0894	.0202	- .0020	.0024	- .0340
0	- 2.00	0	- .0400	.0152	- .0018	.0002	.0014	0	- 2.08	4.00	- .0354	.0136	- .0032	.0015	- .0321
0	- .08	0	- .0028	.0068	- .0019	.0002	- .0002	0	0	4.00	.0007	.0055	- .0032	.0013	- .0323
0	2.00	0	.0336	- .0018	- .0020	.0003	- .0008	0	1.92	4.00	.0387	- .0021	- .0034	.0014	- .0329
0	3.75	0	.0726	- .0063	- .0013	.0003	- .0014	0	3.93	4.00	.0761	- .0063	- .0044	.0007	- .0284
0	5.75	0	.1118	- .0129	- .0014	.0004	- .0010	0	5.76	3.98	.1153	- .0119	- .0036	.0011	- .0291
0	7.92	0	.1583	- .0232	.0001	.0005	- .0006	0	7.69	3.97	.1600	- .0217	- .0040	.0005	- .0301
0	9.83	0	.2073	- .0317	- .0005	.0007	- .0015	0	9.78	3.95	.2078	- .0321	- .0028	.0006	- .0358
0	14.67	0	.3546	- .0658	.0009	.0005	- .0016	0	14.61	3.87	.3543	- .0664	- .0017	.0022	- .0433
0	19.38	0	.5480	- .1234	.0036	.0004	- .0030	0	19.62	3.75	.5452	- .1217	.0007	.0042	- .0516
0	24.25	0	.7843	- .1944	.0056	.0002	- .0044	0	24.38	3.61	.7773	- .1893	.0043	.0062	- .0599
0	- 5.00	1.01	- .0946	.0200	- .0017	- .0002	- .0071	0	- 5.22	7.92	- .0957	.0232	- .0011	.0068	- .0725
0	- 2.17	1.01	- .0393	.0144	- .0030	- .0001	- .0075	0	- 1.92	7.98	- .0377	.0141	- .0033	.0041	- .0675
0	.08	1.00	.0005	.0058	- .0032	.0000	- .0073	0	0	8.01	.0019	.0064	- .0036	.0026	- .0668
0	1.67	1.01	.0368	- .0026	- .0024	- .0001	- .0079	0	1.92	8.01	.0422	- .0016	- .0029	.0023	- .0670
0	3.75	1.00	.0739	- .0081	- .0025	.0002	- .0087	0	3.87	8.00	.0806	- .0080	- .0032	.0018	- .0677
0	5.58	1.00	.1141	- .0136	- .0019	.0003	- .0083	0	5.81	7.98	.1225	- .0139	- .0036	.0019	- .0692
0	7.67	.99	.1599	- .0239	- .0023	.0001	- .0092	0	7.91	7.94	.1671	- .0239	- .0032	.0017	- .0709
0	9.75	.98	.2066	- .0324	- .0018	.0002	- .0103	0	9.93	7.89	.2230	- .0385	- .0032	.0026	- .0750
0	14.58	.97	.3548	- .0663	.0003	.0006	- .0127	0	14.97	7.72	.3724	- .0727	- .0028	.0046	- .0870
0	19.58	.94	.5523	- .1242	.0006	.0011	- .0161	0	19.92	7.50	.5720	- .1242	- .0008	.0074	- .1003
0	24.50	.89	.7972	- .1962	.0040	.0024	- .0203	0	24.71	7.22	.8044	- .1855	.0018	.0100	- .1145

[redacted]

TABLE II.- AERODYNAMIC CHARACTERISTICS OF THE MODELS AT M = 6.86; R = 343,000;

FIVE-COMPONENT BODY-AXIS DATA — Concluded

(b) Body-tail configuration; $\beta = 0^\circ$

i_H, deg.	α, deg.	C_N	C_m	i_H, deg.	α, deg.	C_N	C_m	i_H, deg.	α, deg.	C_N	C_m
10° wedge tails											
0	0.12	0.0002	-0.0008	0	19.55	0.2893	-0.1411	-10	15.00	0.1253	0.0002
0	1.08	.0088	-.0037	0	21.50	.3347	-.1671	-10	19.83	.2068	-.0294
0	2.02	.0163	-.0069	0	23.40	.3778	-.1923	-10	24.58	.3008	-.0684
0	3.03	.0240	-.0099	0	25.35	.4287	-.2214	-20	1.42	-.0598	.1012
0	3.98	.0345	-.0133	0	27.30	.4820	-.2505	-20	2.42	-.0414	.0920
0	4.98	.0438	-.0170	-10	-4.75	-.0754	.0734	-20	4.33	-.0217	.0822
0	5.92	.0545	-.0205	-10	-1.75	-.0435	.0561	-20	6.25	-.0009	.0732
0	7.88	.0767	-.0285	-10	.08	-.0249	.0450	-20	8.83	.0191	.0668
0	9.83	.1020	-.0388	-10	2.17	-.0076	.0372	-20	10.08	.0379	.0655
0	11.87	.1290	-.0512	-10	4.08	.0101	.0296	-20	15.17	.0901	.0620
0	13.82	.1609	-.0678	-10	6.08	.0292	.0243	-20	20.00	.1587	.0539
0	15.70	.2030	-.0897	-10	8.08	.0470	.0198	-20	25.00	.2411	.0324
0	17.68	.2460	-.1151	-10	10.00	.0683	.0157				
Flat-plate tails											
-10	-4.67	-0.0580	0.0424	-10	4.00	0.0152	0.0227	-10	14.75	0.1254	0.0112
-10	-1.83	-.0310	.0322	-10	6.08	.0316	.0210	-10	19.75	.1992	-.0079
-10	.25	-.0161	.0274	-10	8.00	.0481	.0202	-10	24.75	.2870	-.0362
-10	2.08	-.0001	.0244	-10	10.00	.0683	.0184				
10° Flared tails											
-10.4	-4.58	-0.0703	0.0635	-10.4	4.00	0.0127	0.0277	-10.4	14.75	0.1262	0.0070
-10.4	-1.75	-.0407	.0484	-10.4	6.08	.0292	.0241	-10.4	19.75	.2036	-.0179
-10.4	.17	-.0221	.0395	-10.4	8.00	.0481	.0215	-10.4	24.67	.2977	-.0525
-10.4	2.08	-.0048	.0325	-10.4	9.92	.0682	.0188				
20° Flared tails											
-10.2	-4.58	-0.0798	0.0804	-10.2	4.08	0.0098	0.0311	-10.2	14.75	0.1323	-0.0048
-10.2	-1.75	-.0465	.0612	-10.2	6.08	.0289	.0244	-10.2	19.67	.2142	-.0383
-10.2	.33	-.0279	.0488	-10.2	8.00	.0483	.0199	-10.2	20.58	.3142	-.0843
-10.2	2.17	-.0092	.0395	-10.2	9.92	.0710	.0139				
30° Flared tails											
-9.6	-4.59	-0.0872	0.0957	-9.6	3.75	0.0090	0.0323	-9.6	14.50	0.1437	0.0257
-9.6	-2.00	-.0532	.0724	-9.6	5.83	.0303	.0219	-9.6	19.41	.2327	.0726
-9.6	-.17	-.0322	.0569	-9.6	7.75	.0520	.0133	-9.6	24.16	.3408	.1326
-9.6	2.08	-.0112	.0451	-9.6	9.91	.0748	.0046				

[redacted]

TABLE III.- AERODYNAMIC CHARACTERISTICS OF THE MODELS AT M = 6.86; R = 343,000;

TWO-COMPONENT STABILITY-AXIS DATA

(a) Complete model; $\beta = 0^\circ$

i_H, deg.	α, deg.	C_L	C_D	L/D	i_H, deg.	α, deg.	C_L	C_D	L/D	i_H, deg.	α, deg.	C_L	C_D	L/D
10° wedge tails														
0	-0.03	0.0078	0.0374	0.21	0	26.33	0.7362	0.4571	1.61	-10	3.83	0.0441	0.0517	0.85
0	1.80	.0431	.0418	1.03	-10	-5.25	-.1227	.0729	-1.68	-10	4.83	.0569	.0571	.99
0	3.77	.0782	.0487	1.61	-10	-4.25	-.1024	.0644	-1.59	-10	6.00	.0844	.0579	1.45
0	5.93	.1178	.0574	2.05	-10	-2.25	-.0542	.0496	-1.09	-10	8.17	.1259	.0691	1.82
0	8.13	.1618	.0699	2.31	-10	-.17	-.0112	.0459	-.24	-10	10.08	.1597	.0855	1.86
0	10.35	.2091	.0882	2.37	-10	-.08	-.0102	.0422	-.24	-10	15.67	.2936	.1438	2.04
0	15.67	.3564	.1581	2.25	-10	1.92	.0177	.0456	.39	-10	26.00	.6545	.3972	1.64
0	20.78	.5465	.2743	1.99										
Flat-plate tails														
0	-5.25	-0.0869	0.0458	-1.898	0	10.08	0.1802	0.0766	2.351	-10	1.58	0.0148	0.0394	0.3762
0	-4.33	-.0697	.0416	-1.562	0	15.17	.3141	.1336	2.352	-10	3.67	.0450	.0444	1.012
0	-2.25	-.0377	.0385	-.9802	0	20.50	.4887	.2377	2.056	-10	4.75	.0638	.0463	1.379
0	- .25	-.0065	.0349	-.1846	0	25.92	.6918	.3984	1.737	-10	5.67	.0822	.0501	1.641
0	-.17	-.0064	.0344	-.1861	-10	-5.17	-.1099	.0551	-1.993	-10	8.00	.1203	.0603	1.994
0	1.75	.0255	.0379	.6710	-10	-4.75	-.0896	.0506	-1.770	-10	10.17	.1610	.0752	2.141
0	3.92	.0608	.0453	1.342	-10	-2.42	-.0505	.0410	-1.231	-10	15.25	.2884	.1286	2.244
0	4.83	.0752	.0461	1.631	-10	-.42	-.0129	.0364	-.3547	-10	20.58	.4519	.2229	2.026
0	5.83	.0955	.0528	1.807	-10	-.17	-.0129	.0371	-.3501	-10	25.92	.6431	.3712	1.733
0	7.83	.1356	.0622	2.181										
10° Flared tails														
0	-5.33	-0.0929	0.0514	-1.81	-10.2	-4.42	-0.0992	.0588	-1.69	-10.2	4.92	0.0616	0.0504	1.22
0	-.25	-.0063	.0375	-.170	-10.2	-3.33	-.0809	.0538	-1.50	-10.2	5.75	.0812	.0533	1.52
0	5.00	.0818	.0522	1.57	-10.2	-2.25	-.0566	.0477	-1.19	-10.2	7.92	.1190	.0626	1.90
0	10.08	.1891	.0818	2.31	-10.2	-.42	-.0153	.0407	-.375	-10.2	9.92	.1607	.0759	2.12
0	15.17	.3356	.1459	2.30	-10.2	-.17	-.0156	.0397	-.394	-10.2	15.33	.2888	.1320	2.19
0	20.67	.5188	.2590	2.00	-10.2	1.75	.0132	.0426	.310	-10.2	20.58	.4536	.2283	1.99
0	26.00	.7161	.4257	1.68	-10.2	3.67	.0431	.0475	.909	-10.2	25.83	.6471	.3765	1.72
20° Flared tails														
0	-5.50	-0.0988	0.0596	-1.66	-10.2	-4.17	-0.1105	0.0715	-1.55	-10.2	4.92	0.0596	0.0608	0.980
0	.25	-.0089	.0444	-.202	-10.2	-3.33	-.0836	.0636	-1.32	-10.2	5.75	.0824	.0591	1.39
0	4.67	.0815	.0591	1.38	-10.2	-2.25	-.0583	.0546	-1.07	-10.2	7.67	.1219	.0677	1.80
0	10.08	.1918	.0925	2.07	-10.2	-.25	-.0141	.0491	-.288	-10.2	10.00	.1593	.0871	1.83
0	15.25	.3364	.1593	2.11	-10.2	-.17	-.0117	.0446	-.263	-10.2	15.17	.2906	.1437	2.02
0	20.67	.5265	.2769	1.90	-10.2	1.58	.0159	.0483	.329	-10.2	20.42	.4568	.2410	1.90
0	25.92	.7277	.4478	1.62	-10.2	3.58	.0432	.0537	.804	-10.2	25.75	.6523	.3935	1.66
30° Flared tails														
0	-5.33	-0.1050	0.0673	-1.56	-9.6	-4.33	-0.1163	0.0800	-1.45	-9.6	5.75	0.0844	0.0686	1.23
0	-.17	-.0116	.0469	- .248	-9.6	-3.25	-.0919	.0744	-1.24	-9.6	7.75	.1300	.0775	1.68
0	4.83	.0824	.0665	1.239	-9.6	-2.17	-.0583	.0632	-.922	-9.6	9.92	.1629	.0916	1.78
0	10.17	.1989	.1019	1.952	-9.6	-.25	-.0141	.0514	-.226	-9.6	15.25	.2942	.1503	1.96
0	15.33	.3512	.1742	2.016	-9.6	1.75	.0193	.0538	.359	-9.6	20.58	.4642	.2521	1.84
0	20.67	.5446	.2994	1.819	-9.6	3.75	.0418	.0629	.665	-9.6	25.50	.6657	.4079	1.63
0	25.83	.7374	.4778	1.544	-9.6	4.83	.0541	.0647	.837					
X-Tail configuration														
0	0	-0.0007	0.0443	-0.02	0	4	0.0630	0.0491	1.28	0	8	0.1396	0.0674	2.07
0	1	.0138	.0448	.31	0	5	.0817	.0523	1.56	0	9	.1616	.0742	2.18
0	2	.0299	.0453	.66	0	6	.1003	.0563	1.78	0	10	.1853	.0827	2.24
0	3	.0454	.0466	.98	0	7	.1174	.0611	1.92					

[redacted]

TABLE III.- AERODYNAMIC CHARACTERISTICS OF THE MODELS AT M = 6.86; R = 343,000;

TWO-COMPONENT STABILITY-AXIS DATA – Concluded

(b) Body-tail configuration; $\beta = 0^\circ$

i_H, deg.	α, deg.	C_L	C_D	L/D	i_H, deg.	α, deg.	C_L	C_D	L/D	i_H, deg.	α, deg.	C_L	C_D	L/D
10° wedge tails														
-20	5.83	-0.0082	0.0433	-0.18	-20	-0.08	-0.0661	.0543	-1.21	-20	-4.08	-0.1092	0.0755	-1.44
-20	4.00	-.0292	.0444	-.65	-20	-1.92	-.0867	.0635	-1.36	-20	-5.00	-.1213	.0827	-1.46
-20	1.92	-.0482	.0486	-.99										
Flat-plate tails														
0	-5.25	-0.0431	0.0237	-1.82	0	20.08	0.2182	0.1149	1.90	-10	9.83	0.0610	0.0388	1.57
0	-.17	-.0064	.0197	-.33	0	24.92	.2997	.1795	1.67	-10	14.92	.1178	.0618	1.90
0	4.83	.0281	.0239	1.18	-10	-5.25	-.0621	.0349	-1.78	-10	19.92	.1777	.0716	2.48
0	9.75	.0733	.0378	1.94	-10	-.17	-.0196	.0259	-.75	-10	25.00	.2485	.1547	1.61
0	14.75	.1372	.0654	2.10	-10	4.83	.0177	.0273	.65					
10° Flared tails														
0	-5.08	-0.0431	0.0281	-1.53	0	20.00	0.2321	0.1267	1.83	-10.4	9.92	0.0608	0.0362	1.68
0	-.17	-.0077	.0248	-.313	0	25.17	.3203	.2025	1.58	-10.4	15.00	.1148	.0617	1.86
0	4.92	.0319	.0288	1.11	-10.4	-5.33	-.0672	.0384	-1.75	-10.4	19.92	.1831	.1014	1.81
0	9.75	.0812	.0440	1.85	-10.4	-.17	-.0218	.0274	-.796	-10.4	25.00	.2582	.1595	1.62
0	15.08	.1458	.0750	1.94	-10.4	4.83	.0172	.0276	.622					
20° Flared tails														
0	-5.17	-0.0491	0.0310	-1.58	0	20.17	0.2507	0.1436	1.75	-10.2	10.00	0.0641	0.0440	1.46
0	-.25	-.0053	.0266	-.20	0	25.08	.3438	.2239	1.54	-10.2	15.08	.1215	.0687	1.77
0	4.92	.0356	.0316	1.13	-10.2	-5.25	-.0785	.0477	-1.64	-10.2	20.25	.1911	.1119	1.71
0	9.83	.0869	.0480	1.80	-10.2	-.33	-.0270	.0335	-.81	-10.2	25.17	.2751	.1763	1.56
0	15.08	.1603	.0844	1.89	-10.2	4.92	.0156	.0326	.48					
30° Flared tails														
0	-5.25	-0.0538	0.0389	-1.38	0	20.17	0.2808	0.1739	1.61	-9.6	9.83	0.0602	0.0513	1.17
0	-.17	-.0038	.0320	-.12	0	25.33	.3770	.2672	1.41	-9.6	14.92	.1235	.0796	1.55
0	5.00	.0442	.0393	1.12	-9.6	-5.42	-.0934	.0629	-1.48	-9.6	20.00	.2026	.1290	1.57
0	10.08	.1048	.0607	1.73	-9.6	-.21	-.0405	.0431	-.94	-9.6	25.00	.2909	.2000	1.45
0	15.08	.1830	.1040	1.76	-9.6	4.58	.0088	.0398	.22					

[redacted]

TABLE IV.- AERODYNAMIC CHARACTERISTICS OF THE MODELS AT M = 6.86; R = 343,000; ONE-COMPONENT BALANCE DATA

(a) Complete model; $\beta = 0^\circ$

i_H, deg.	α, deg.	C_m	i_H, deg.	α, deg.	C_m	i_H, deg.	α, deg.	C_m
30° Flared tails								
-9.6	-5	0.0864	-9.6	2	0.0142	-9.6	10	-0.0041
-9.6	-2	.0401	-9.6	4	.0274	-9.6	15	-.0302
-9.6	0	.0116	-9.6	5	.0248			

(b) Body-tail configuration; $\beta = 0^\circ$

10° wedge tails								
-20	-5	0.1475	-20	0	0.1073	-20	4	0.0843
-20	-4	.1383	-20	2	.0945	-20	6	.0762
-20	-2	.1215						
Flat-plate tails								
0	-5	0.004	0	5	-0.003	0	15	-0.038
0	0	.002	0	10	-.014			
10° Flared tails								
0	-5	0.0105	0	5	-0.0124	0	15	-0.0659
0	0	-.0009	0	10	-.0310			
20° Flared tails								
0	-5	0.0186	0	5	-0.0194	0	15	-0.0960
0	0	.0020	0	10	-.0471			
30° Flared tails								
0	-5	0.0276	0	5	-0.0325	0	15	-0.1313
0	0	-.0010	0	10	-.0733			

[redacted]

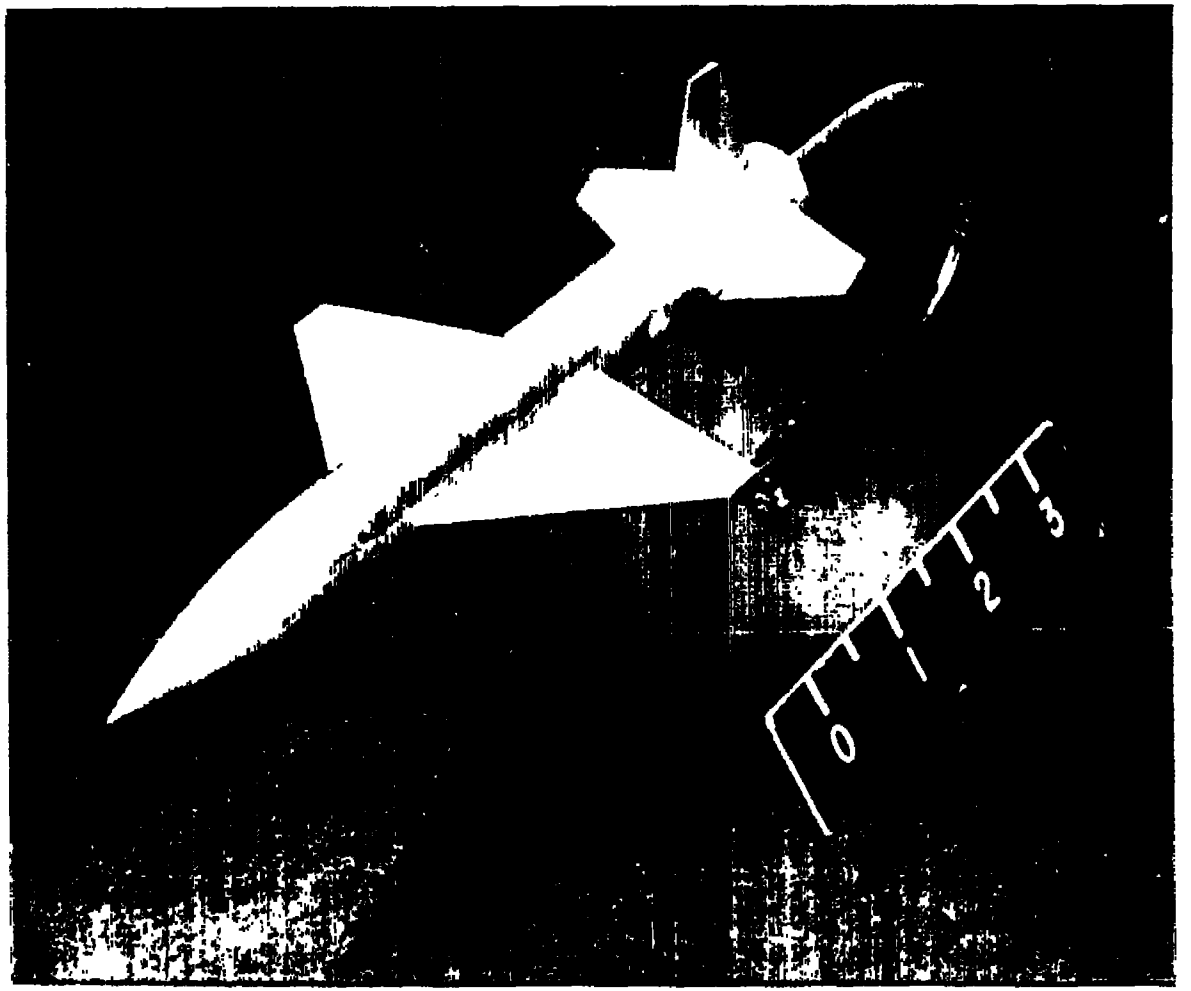

L-88000

Figure 1.- Photograph of complete model with 10° wedge tail sections. $i_H = -20°$.

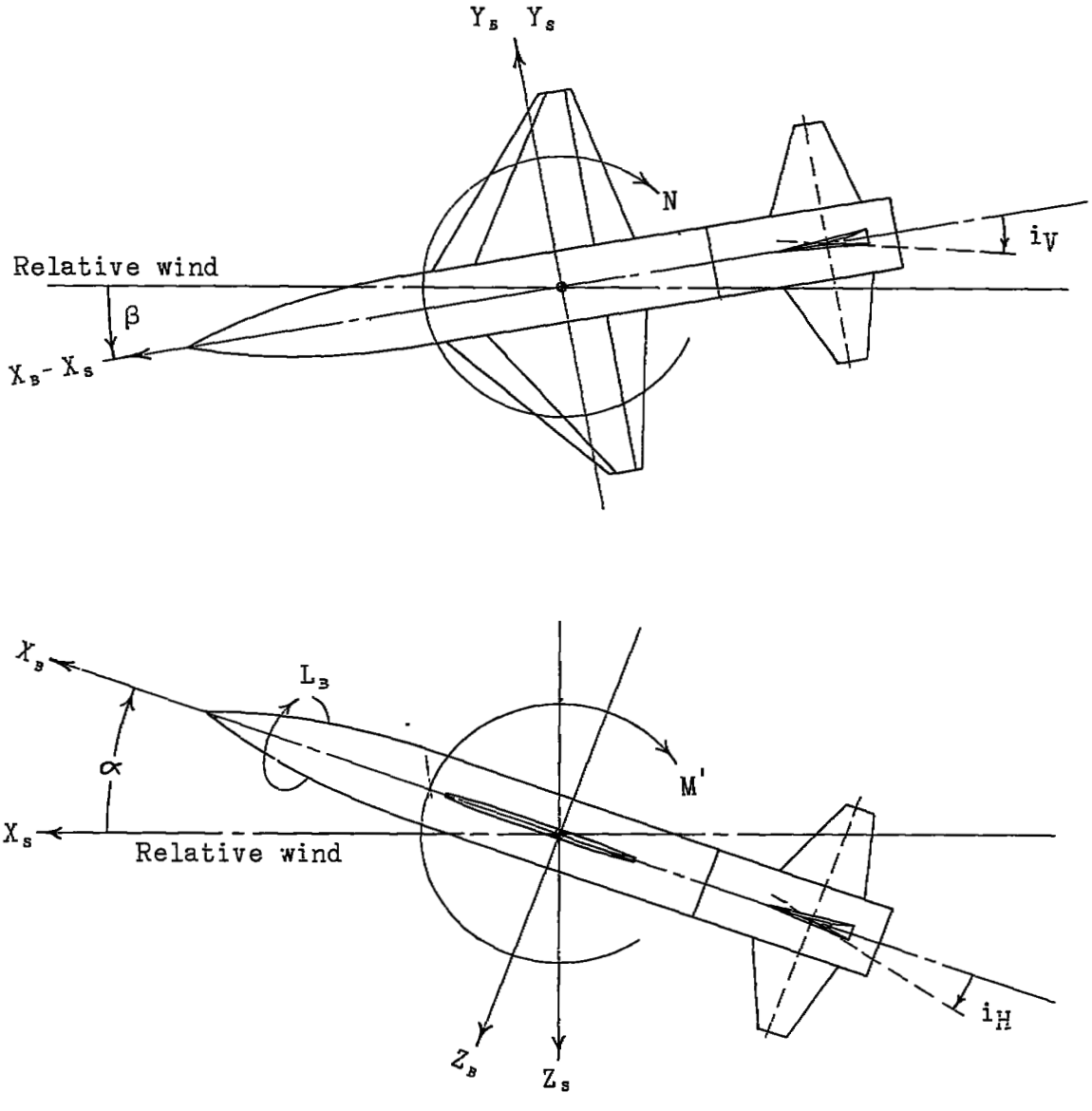

Figure 2.- Systems of reference axes. Arrows indicate positive direction.

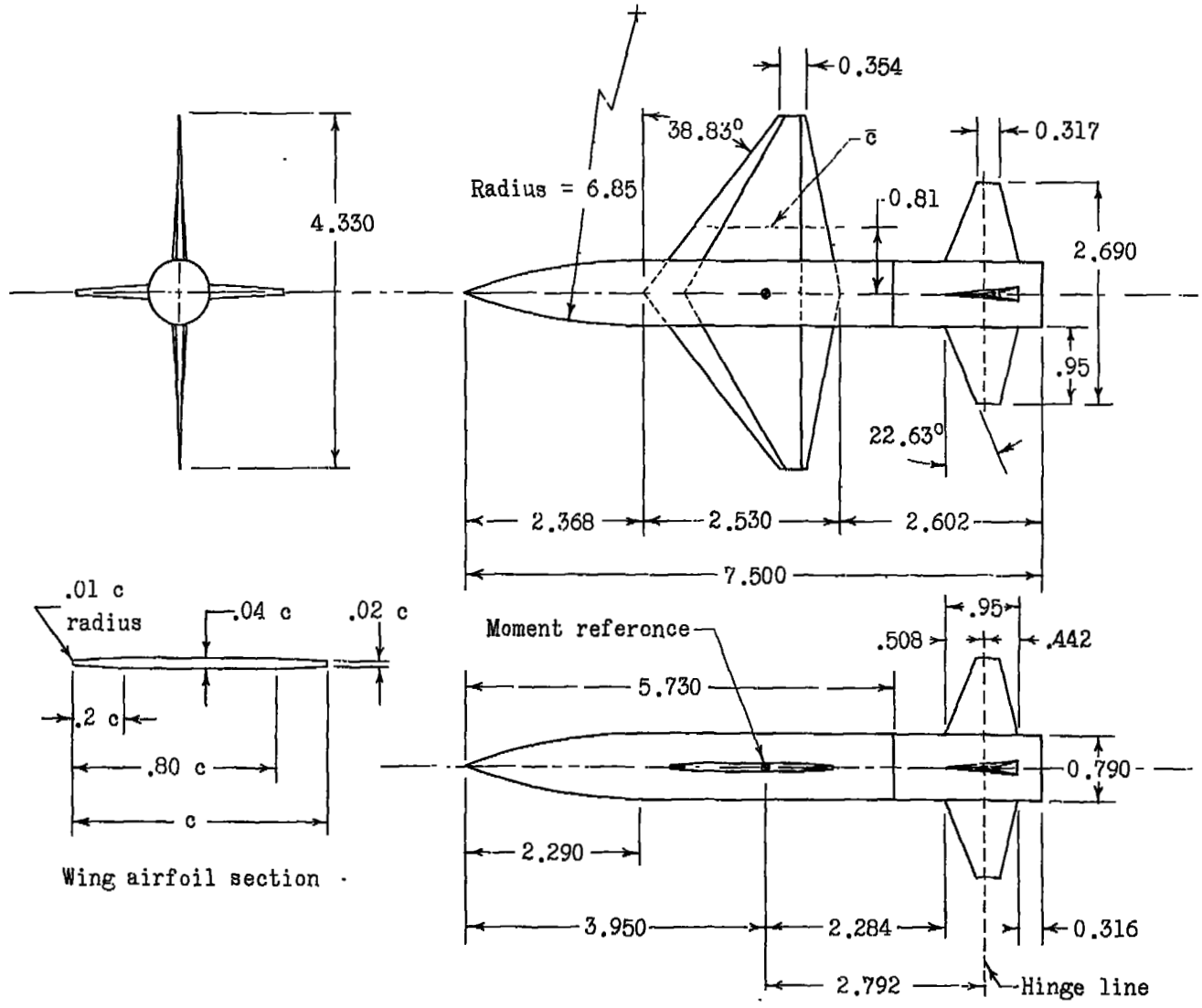

Figure 3.- Wind-tunnel model. All dimensions in inches.

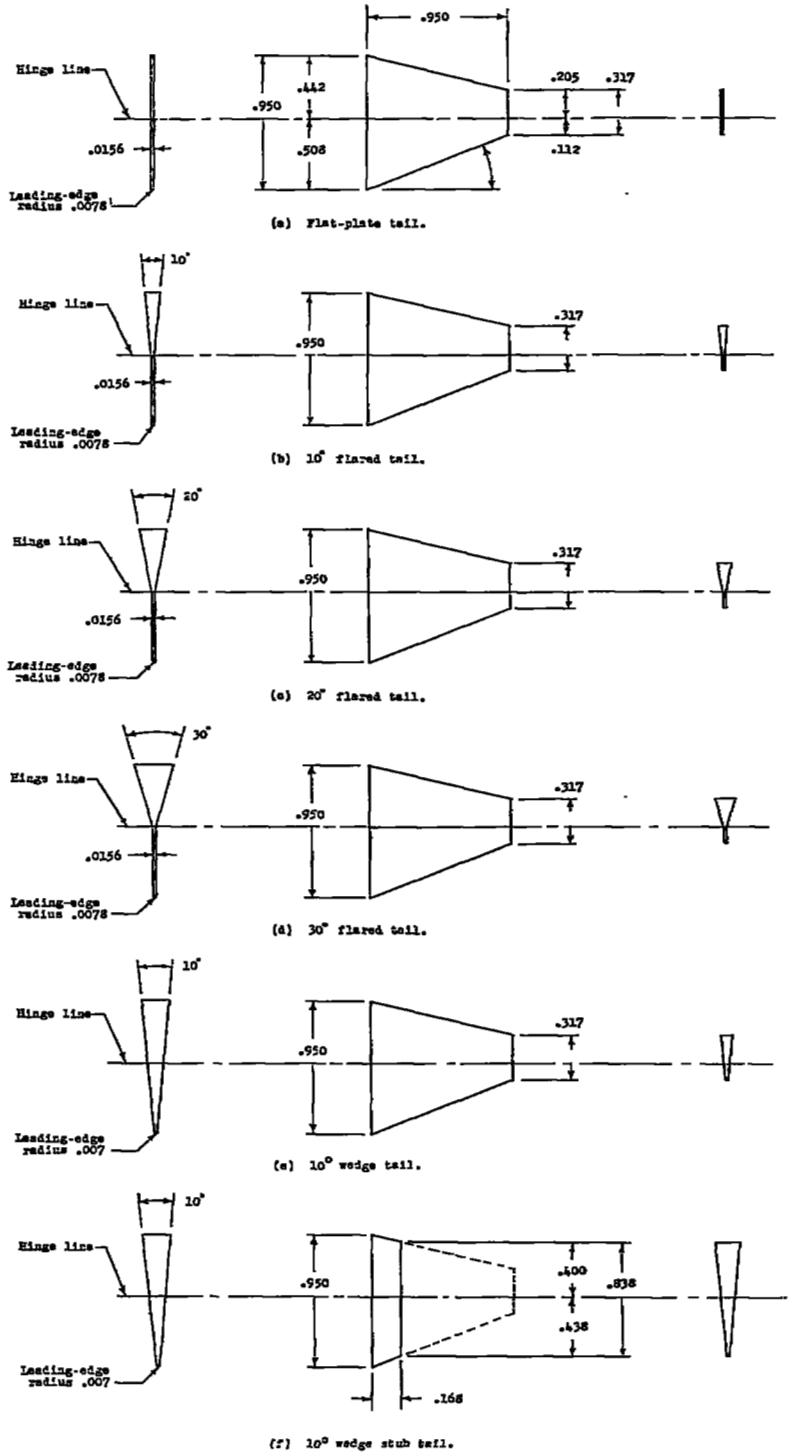

Figure 4.- Details of the airfoil sections and exposed plan forms of the various tails tested.

[redacted]

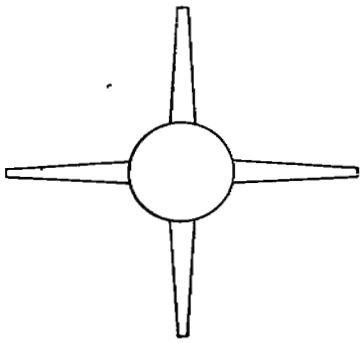

Complete model

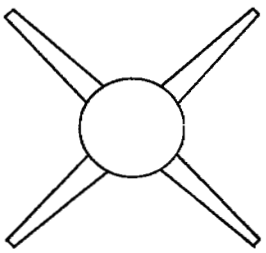

X- Tail configuration

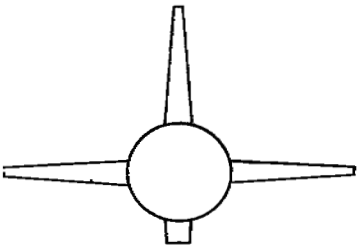

Stub-tail configuration

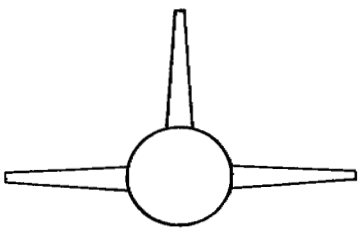

Horizontal tail and top vertical tail

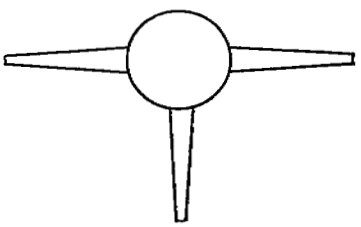

Horizontal tail and bottom vertical tail

Figure 5.- Tail configurations tested.

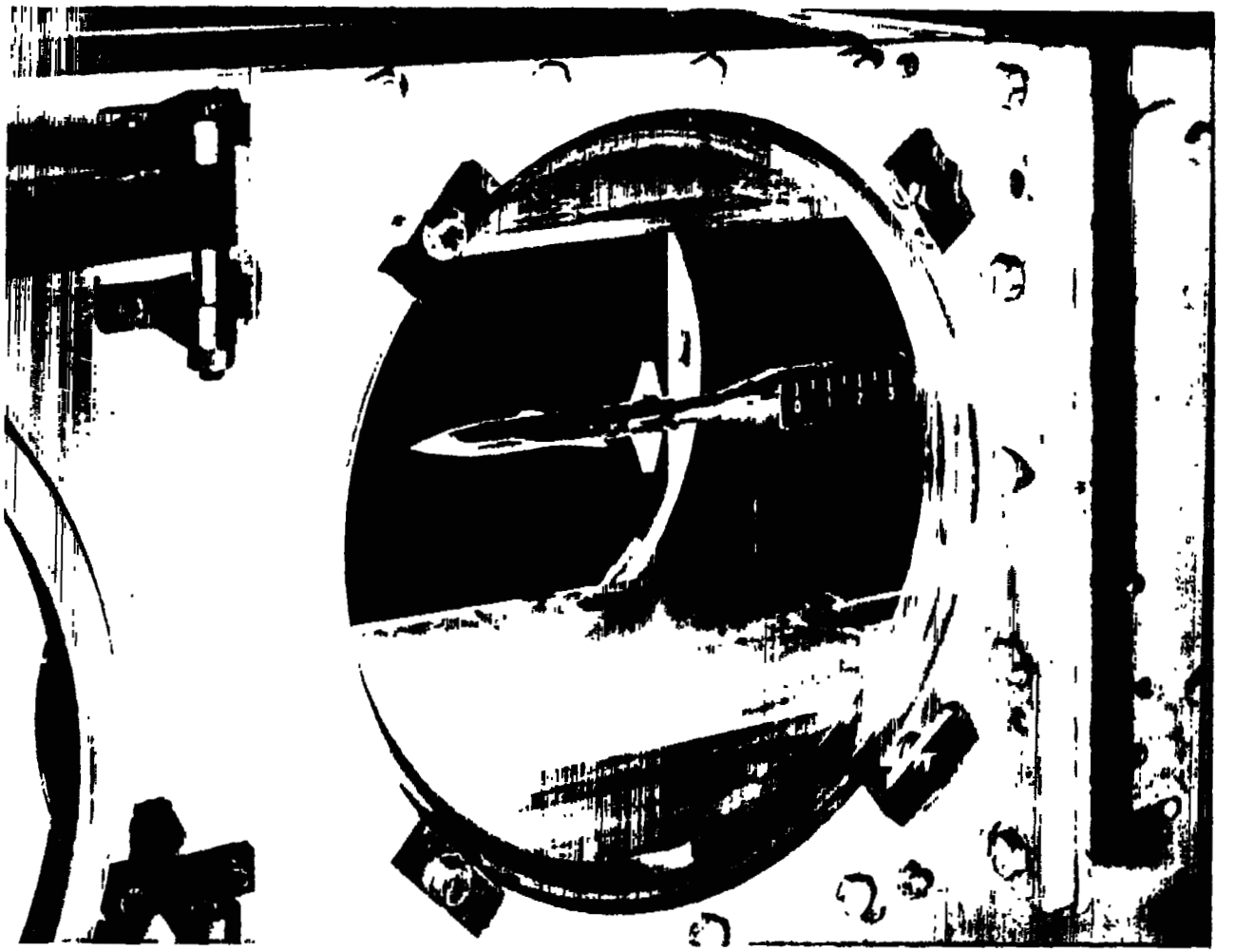

L-86712

Figure 6.- Installation of model in the Langley 11-inch hypersonic tunnel. $\alpha = 0^{\circ}$; $\beta = 0^{\circ}$.

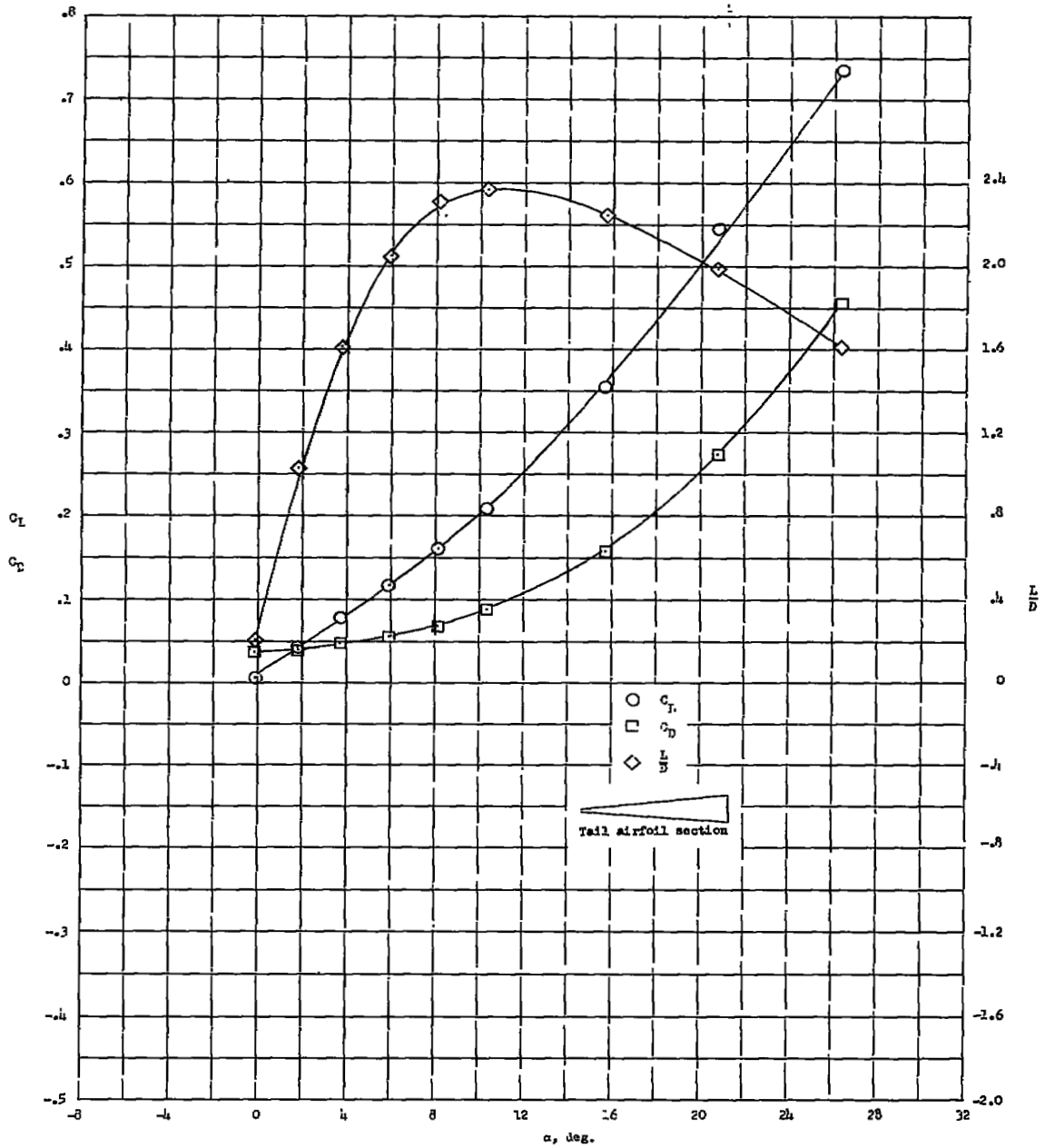

(a) 10° wedge tails; β = 0°.

Figure 7.- Variation of lift coefficient, drag coefficient, and lift-drag ratio with angle of attack for the complete model configuration with various tail airfoil sections. i_H = 0°; M = 6.86; R = 343,000; stability-axis data.

[redacted]

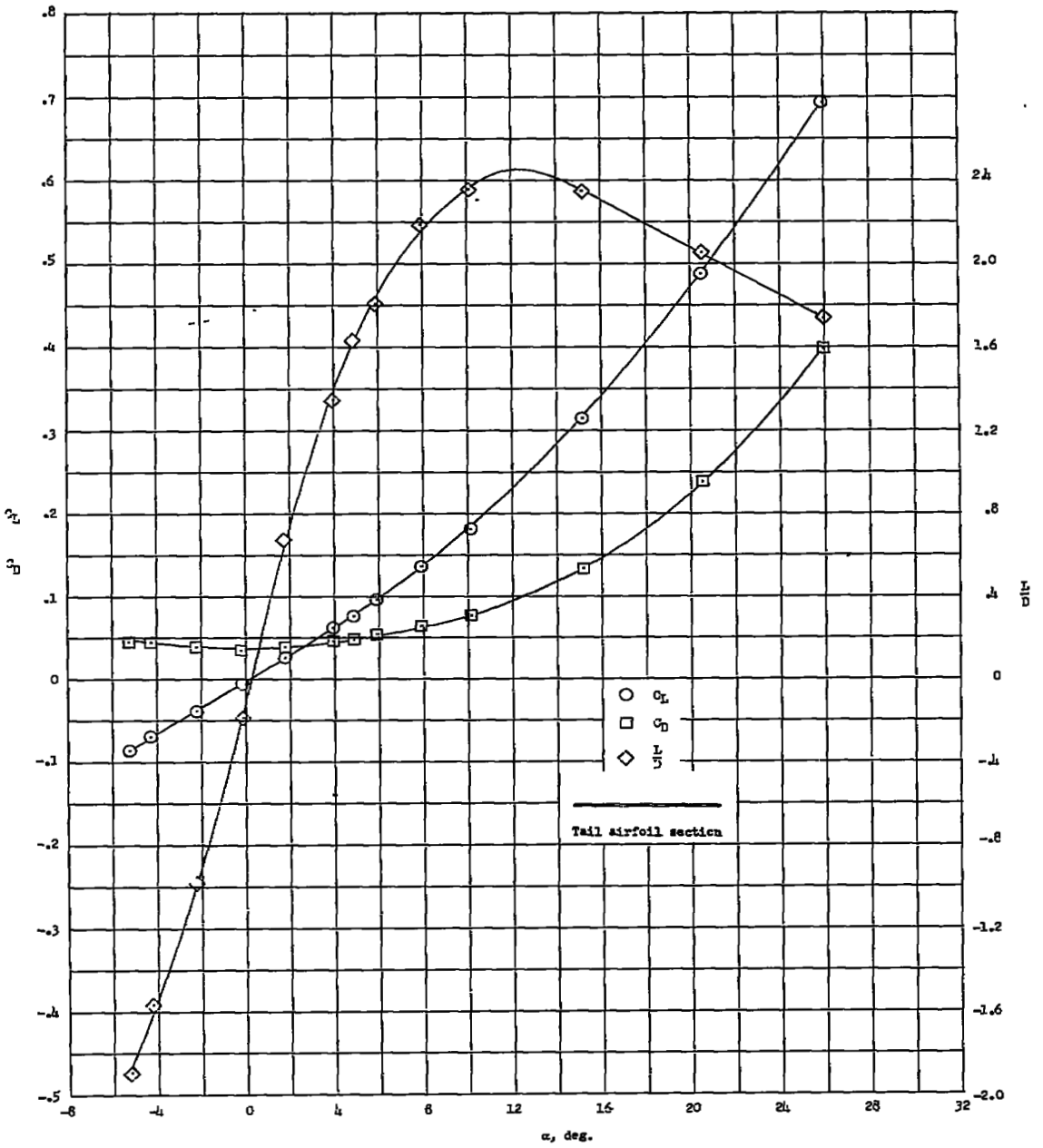

(b) Flat-plate tails; $\beta = 0^{\circ}$.

Figure 7.- Continued.

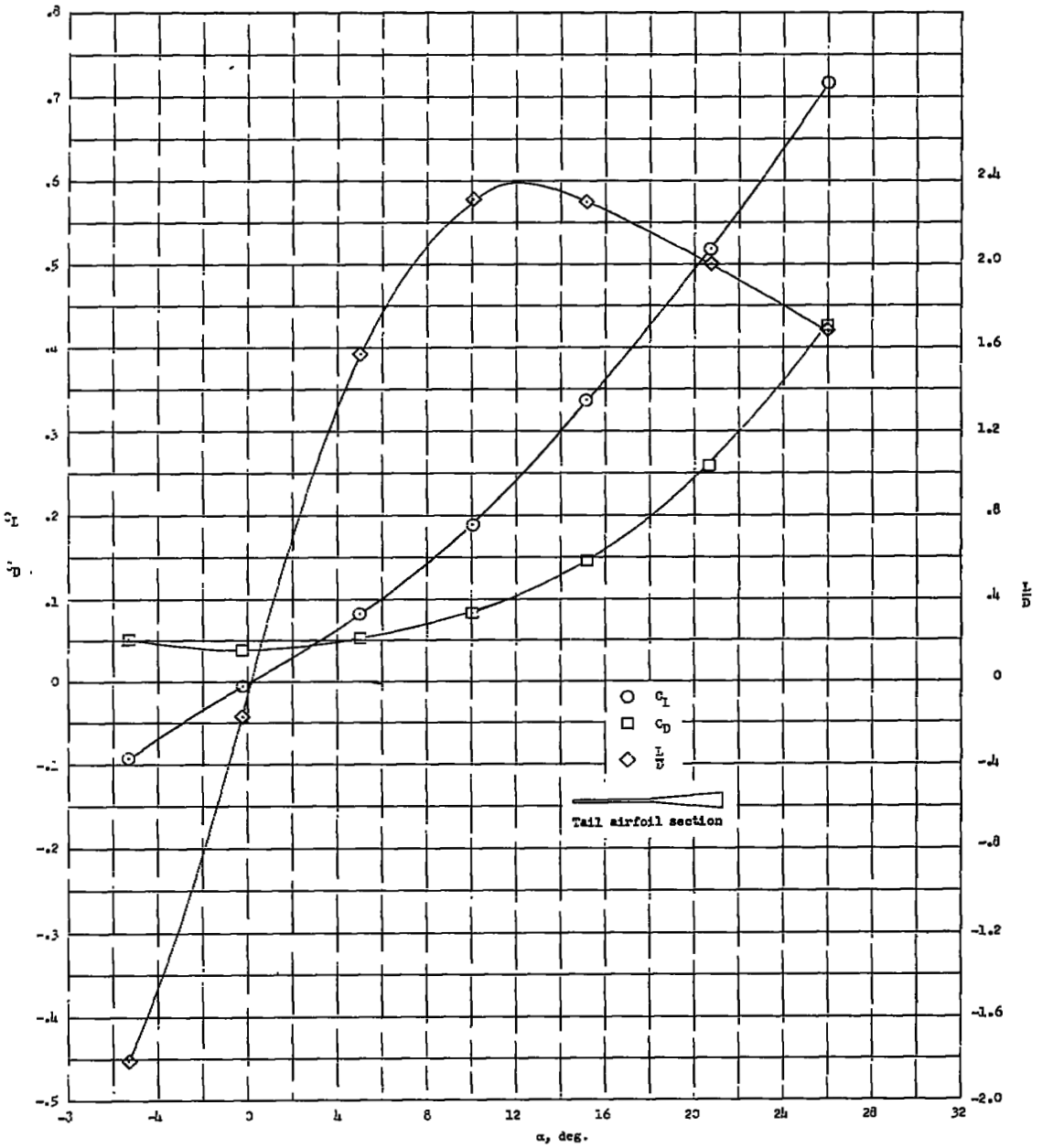

(c) 10° flared tails; β = 0°.

Figure 7.- Continued.

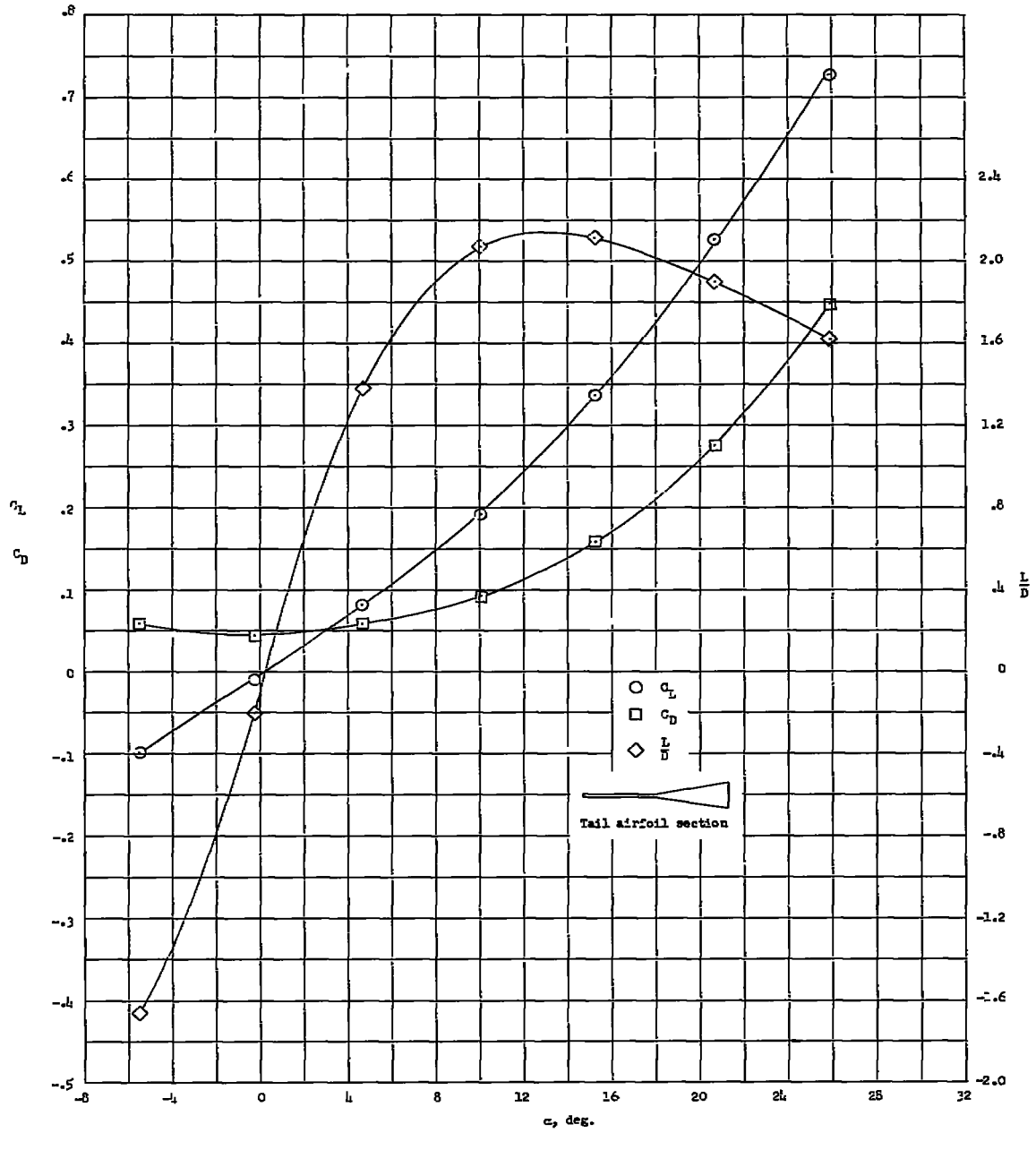

(d) 20° flared tails; $\beta = 0°$.

Figure 7.- Continued.

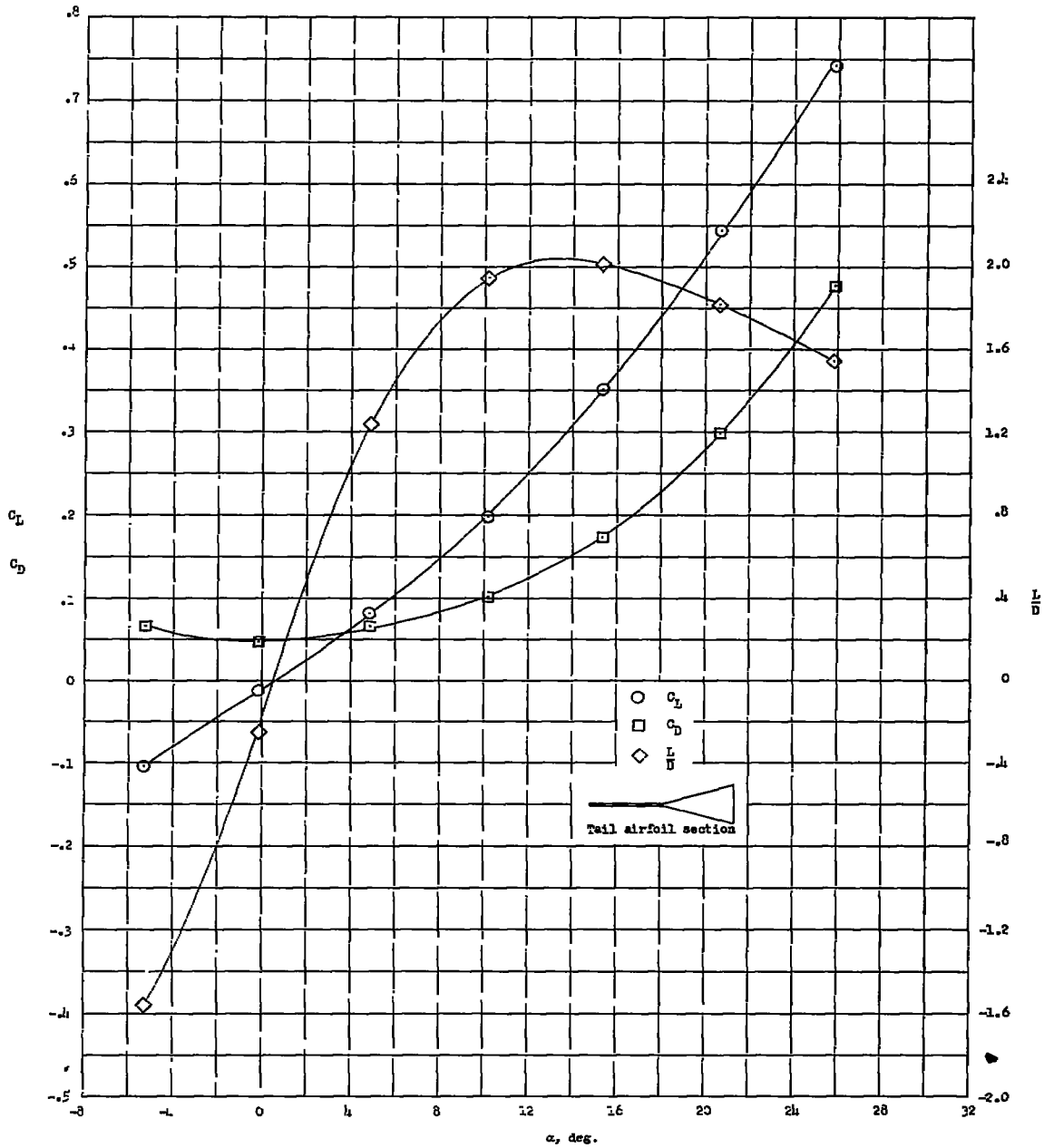

(e) 30° flared tails; $\beta = 0°$.

Figure 7.- Concluded.

[redacted]

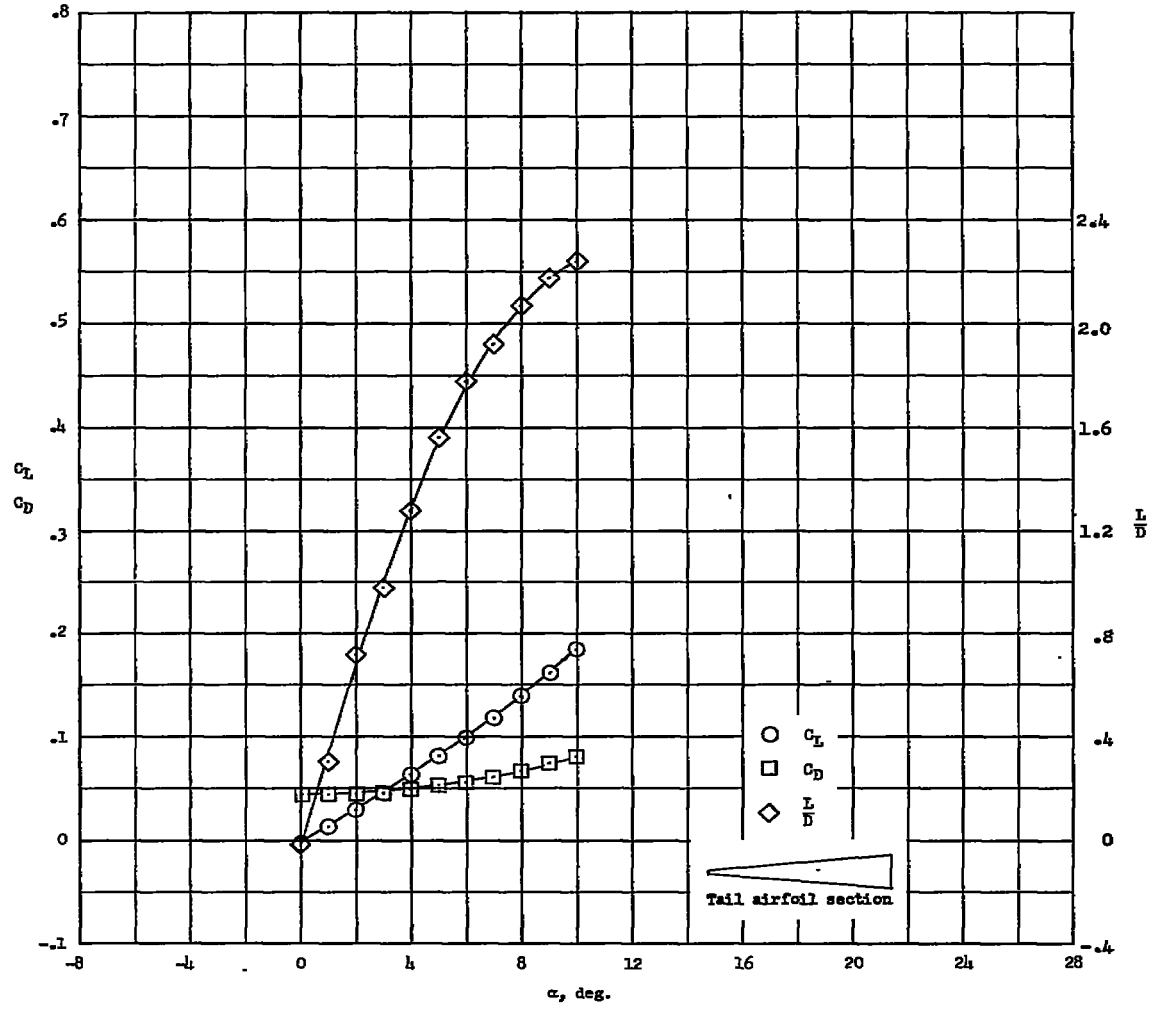

Figure 8.- Variation of lift coefficient, drag coefficient, and lift-drag ratio with angle of attack for the complete model using the X-tail configuration with 10° wedge tail airfoil sections. M = 6.86; R = 343,000; stability-axis data; $\beta = 0^\circ$.

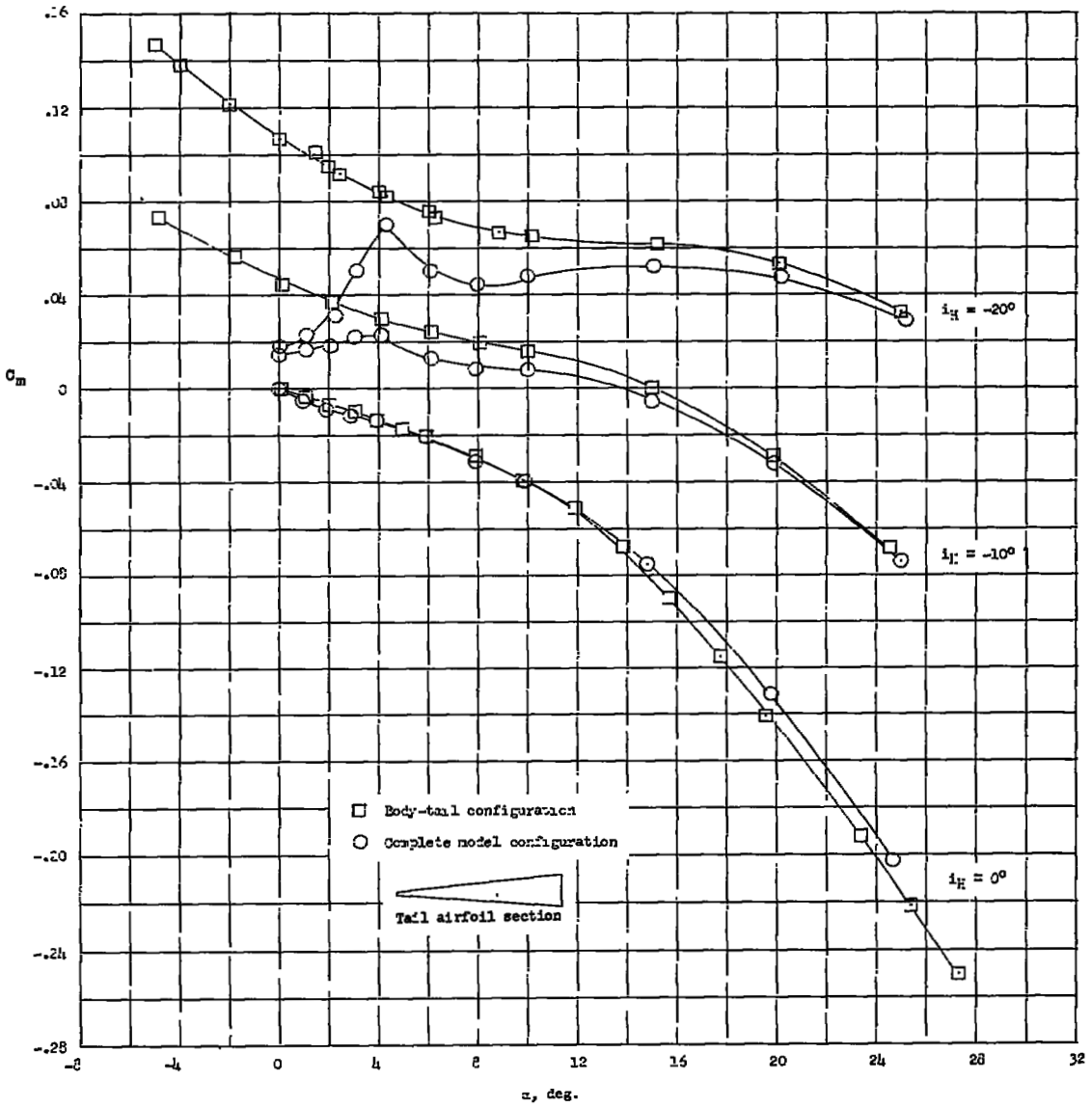

(a) 10° wedge tail; β = 0°.

Figure 9.- Variation of pitching-moment coefficient with angle of attack for the complete model and body-tail configurations with various tail airfoil sections. M = 6.86; R = 343,000; stability-axis data.

[redacted]

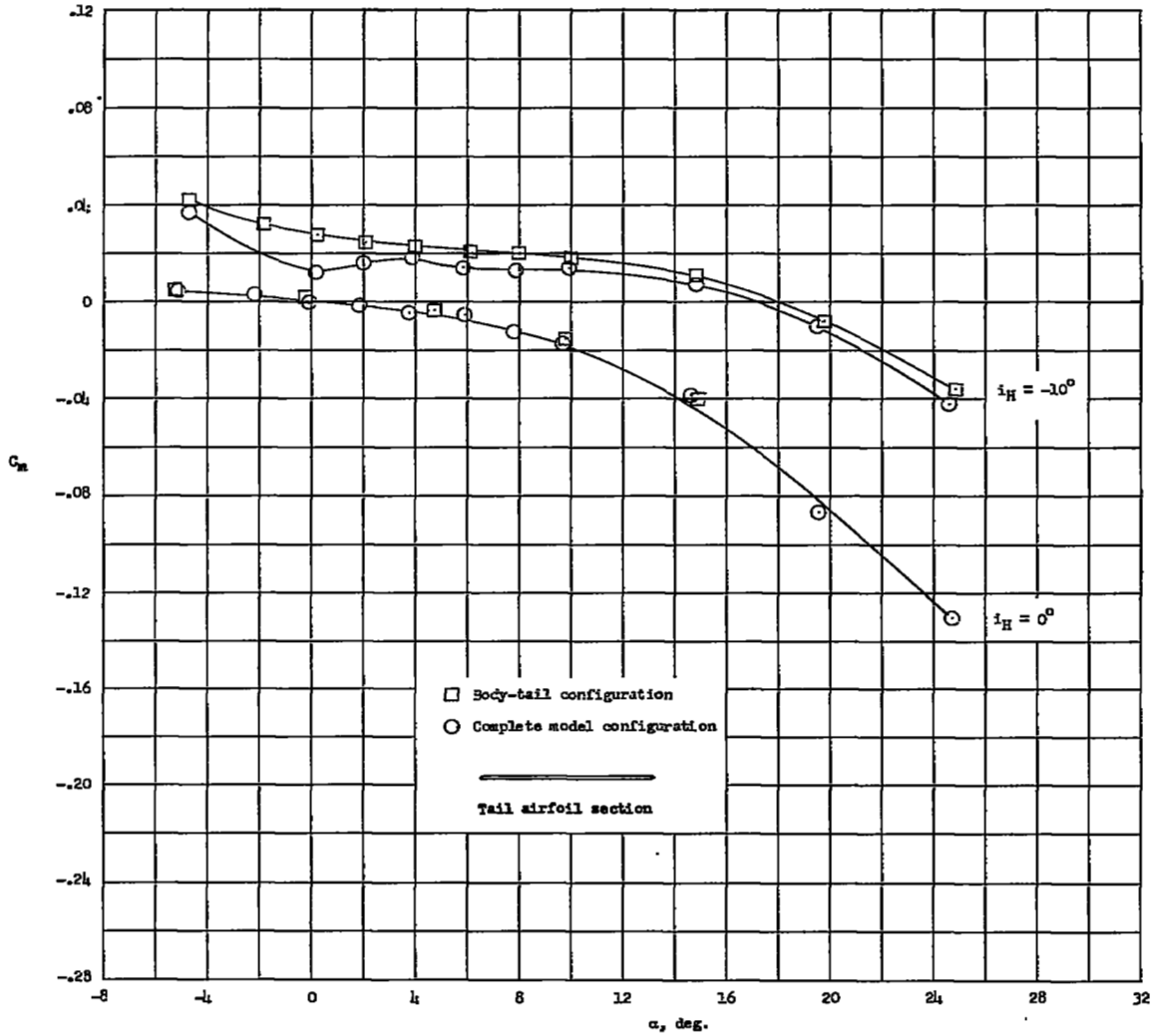

(b) Flat-plate tails; $\beta = 0°$.

Figure 9.- Continued.

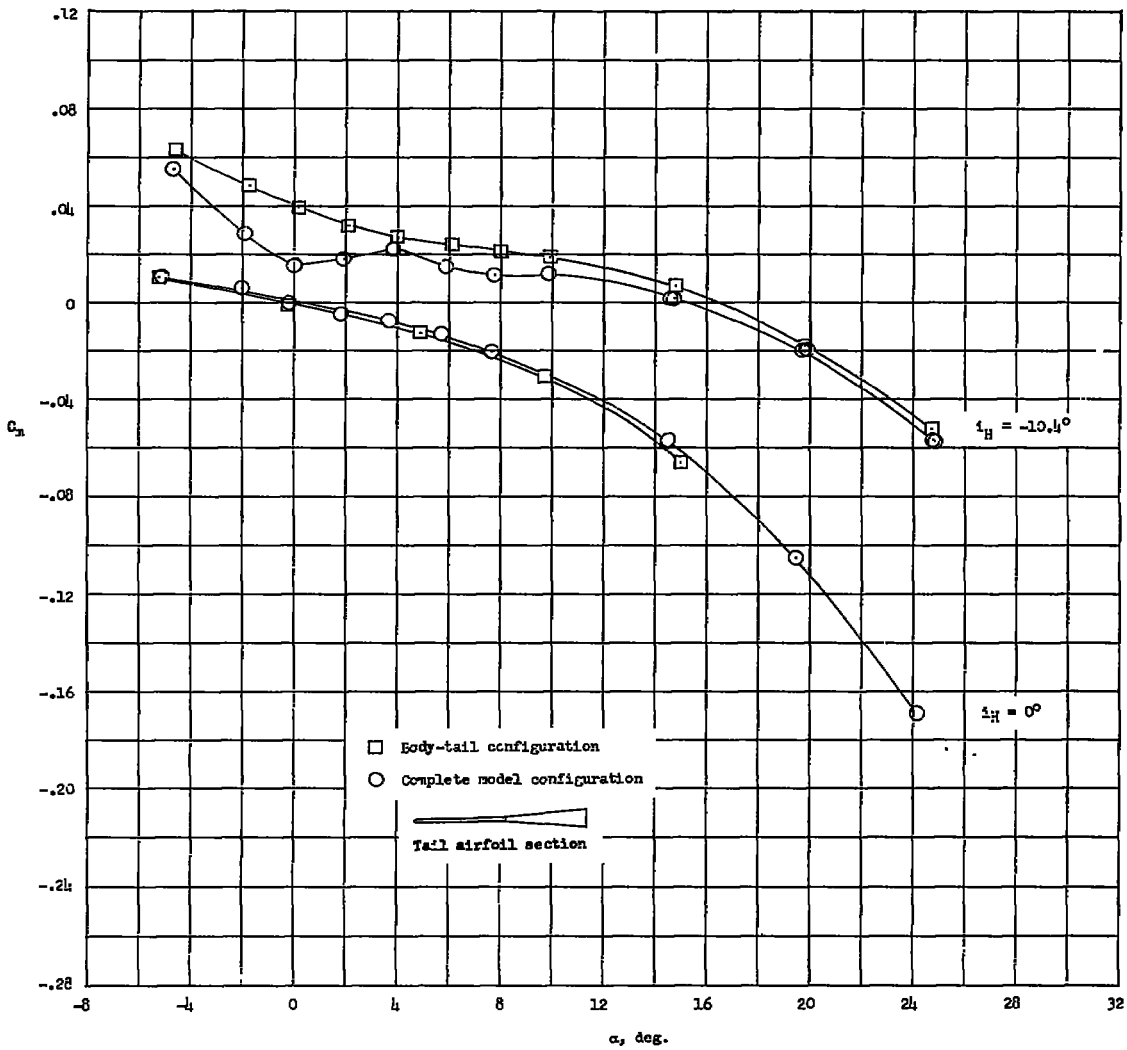

(c) 10° flared tails; β = 0°.

Figure 9.- Continued.

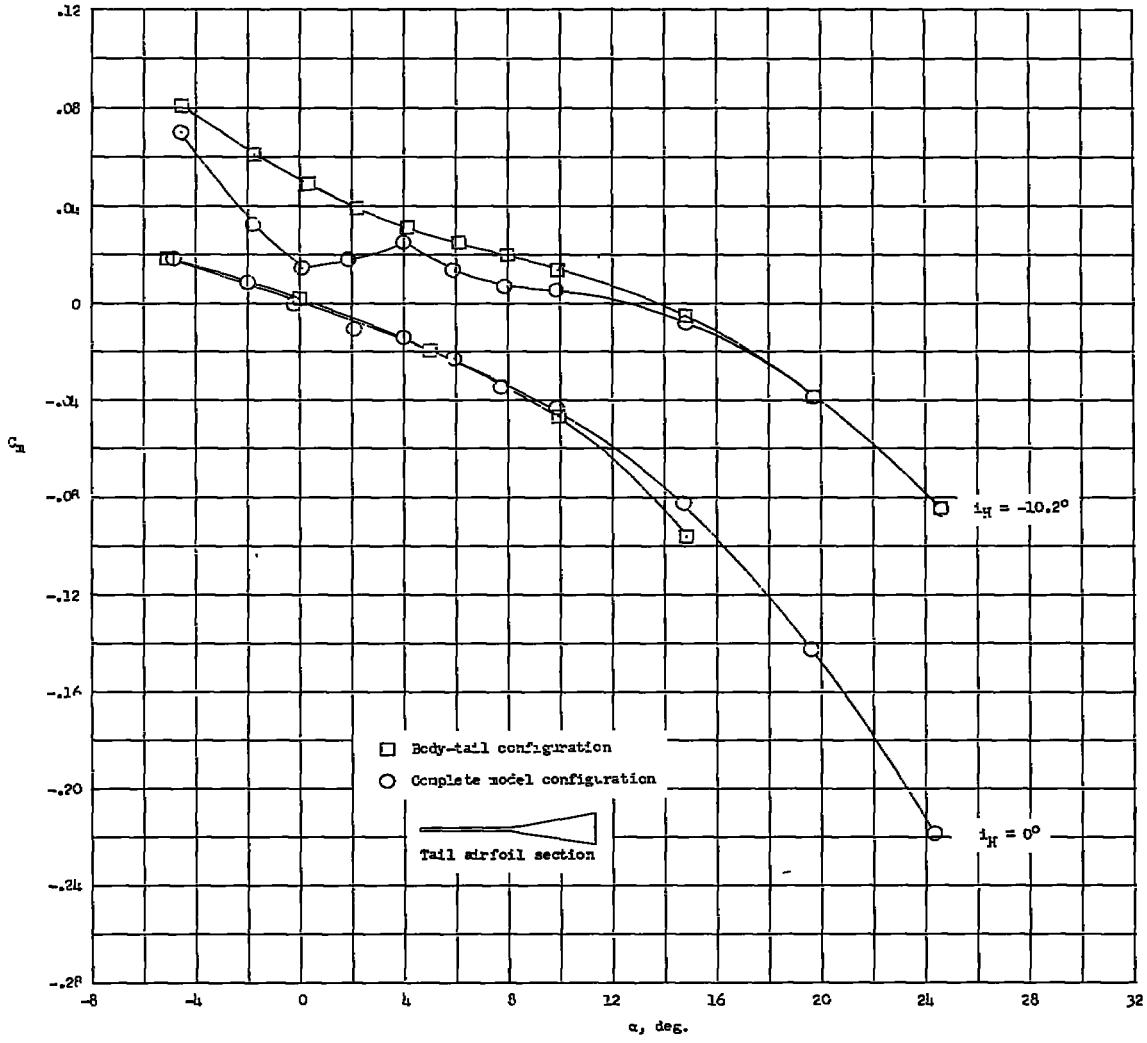

(d) 20° flared tails; $\beta = 0°$.

Figure 9.- Continued.

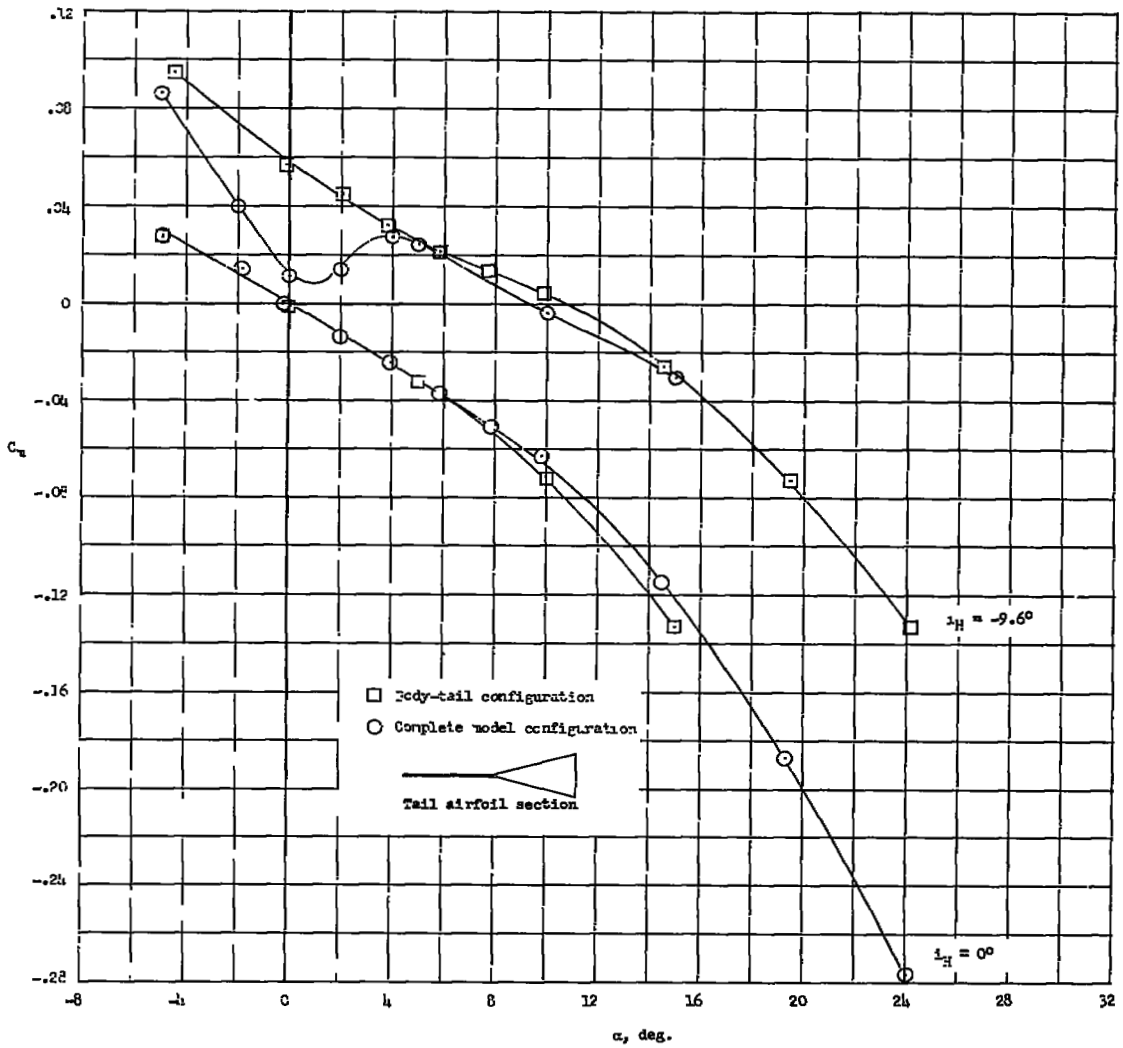

(e) 30° flared tails; $\beta = 0°$.

Figure 9.- Concluded.

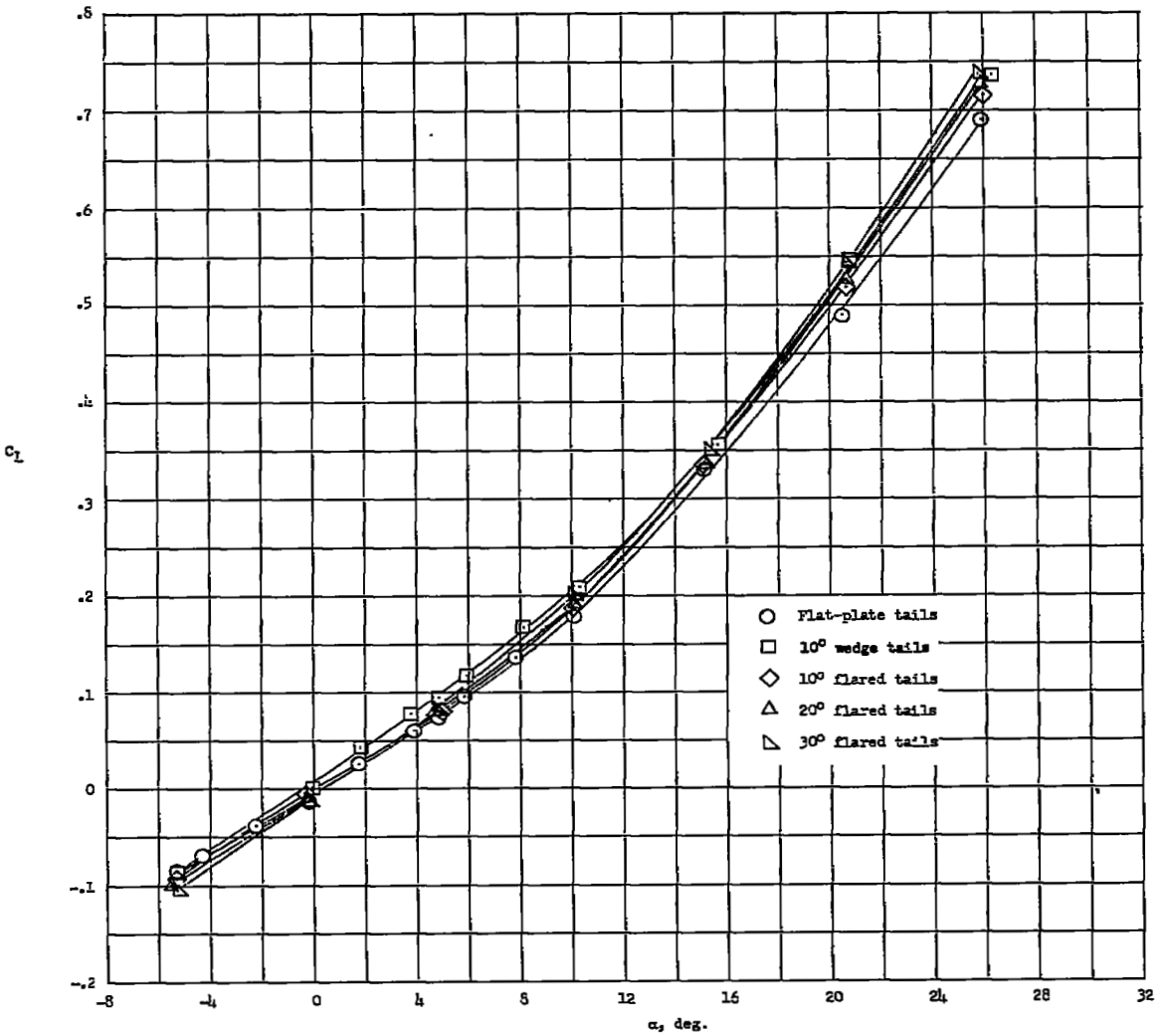

(a) $i_H = 0^\circ$; $\beta = 0^\circ$.

Figure 10.- Effect of tail airfoil section on the variation of lift coefficient with angle of attack for the complete model configuration. M = 6.86; R = 343,000; stability-axis data.

[redacted]

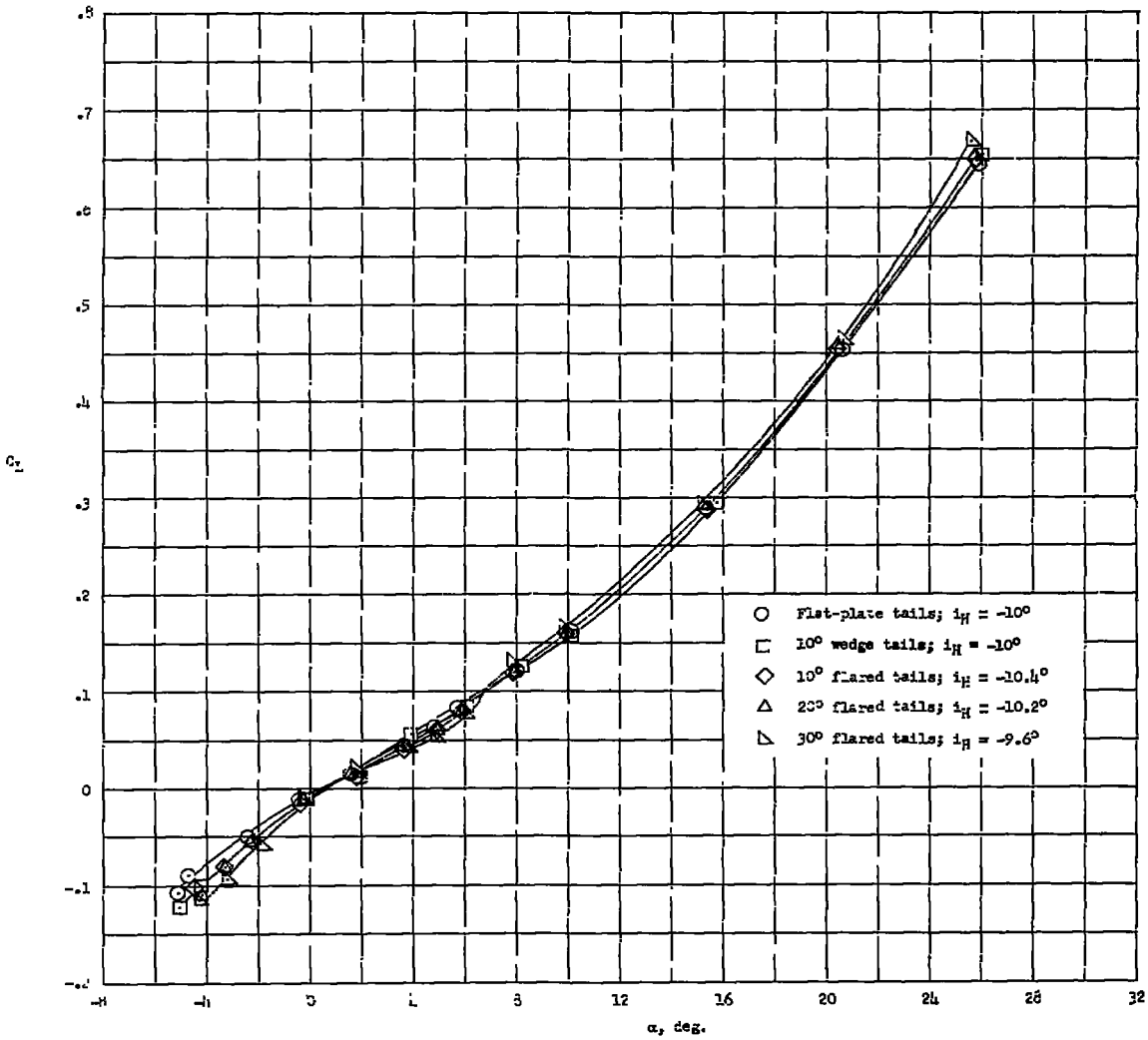

(b) $i_H \approx -10^\circ$; $\beta = 0^\circ$.

Figure 10.- Concluded.

[redacted]

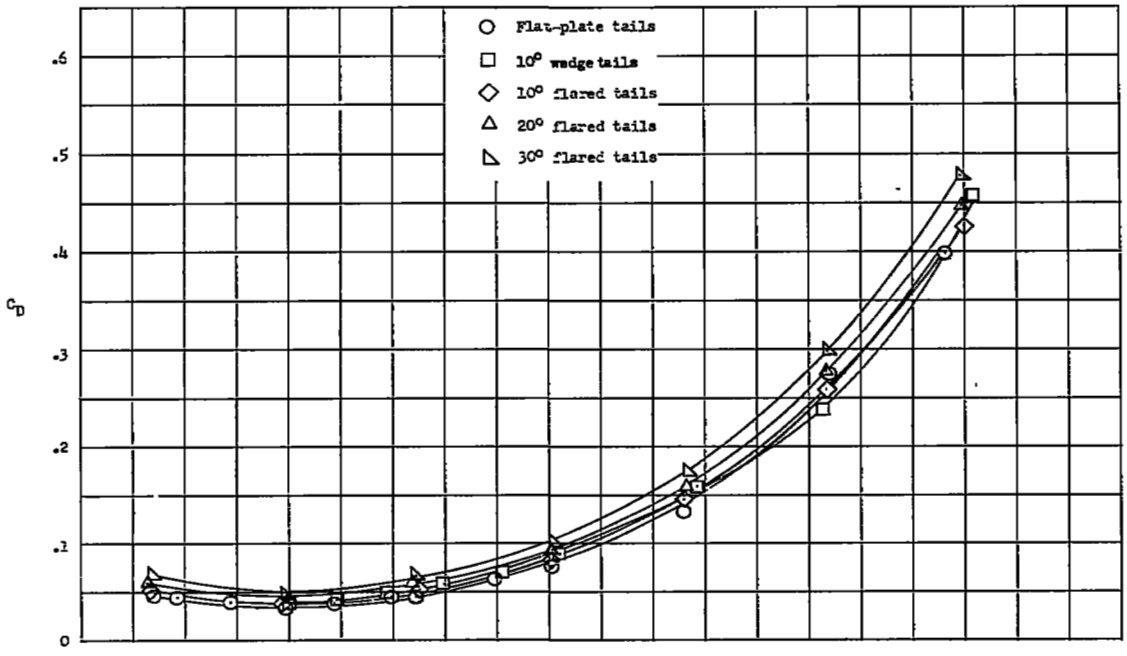

(a) $I_H = 0^\circ$; $\beta = 0^\circ$.

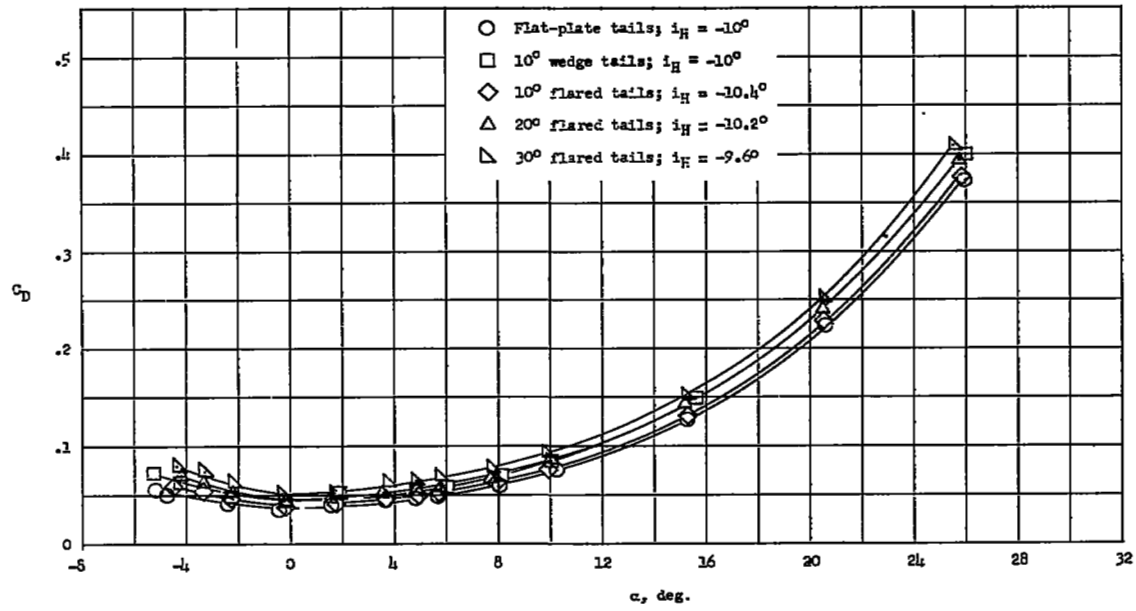

(b) $I_H \approx -10^\circ$; $\beta = 0^\circ$.

Figure 11.- Effect of tail airfoil section on the variation of drag coefficient with angle of attack for the complete model configuration. M = 6.86; R = 343,000; stability-axis data.

[redacted]

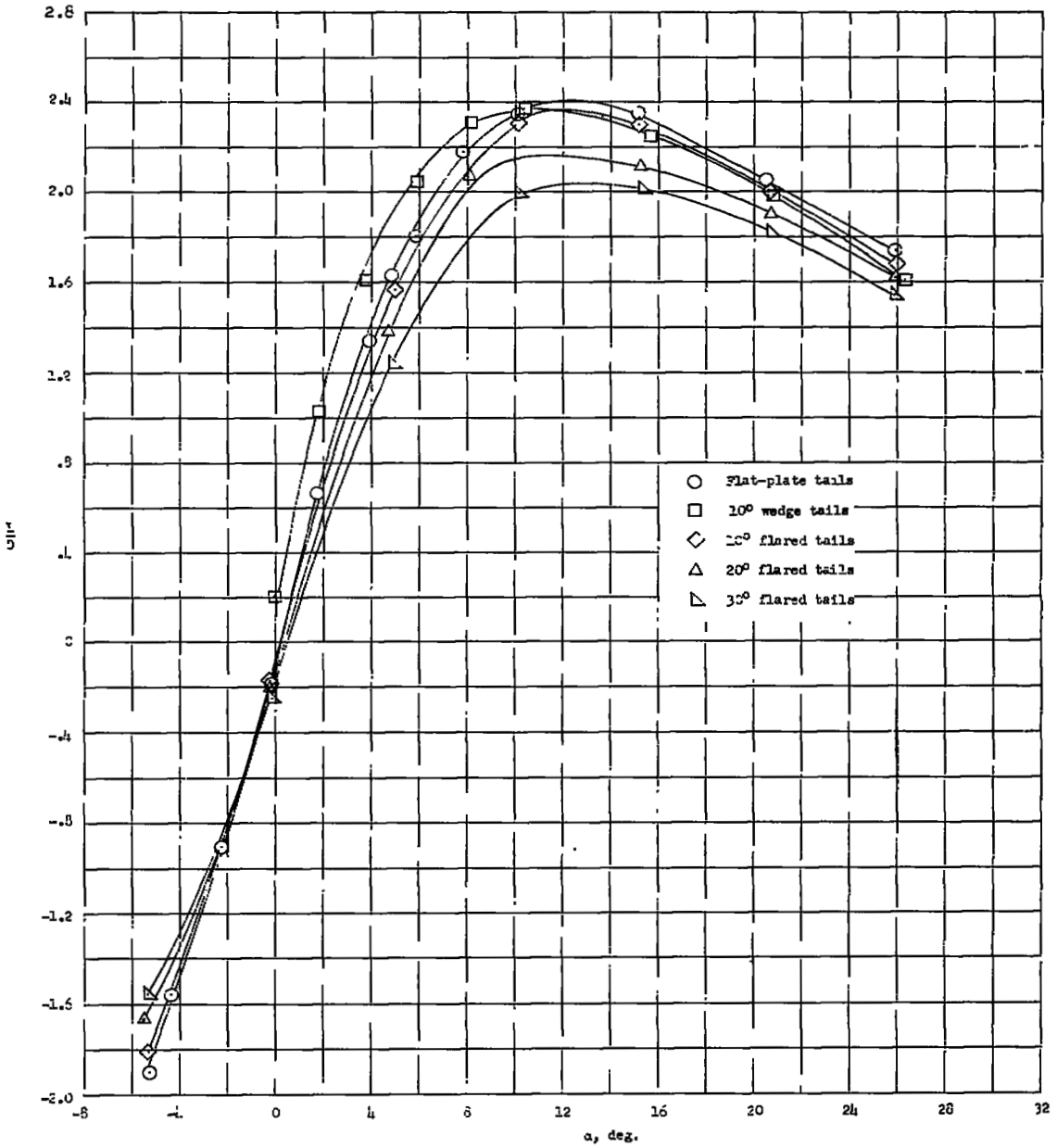

(a) $i_H = 0^\circ$; $\beta = 0^\circ$.

Figure 12.- Effect of tail airfoil section on the variation of lift-drag ratio with angle of attack for the complete model configuration. M = 6.86; R = 343,000; stability-axis data.

[redacted]

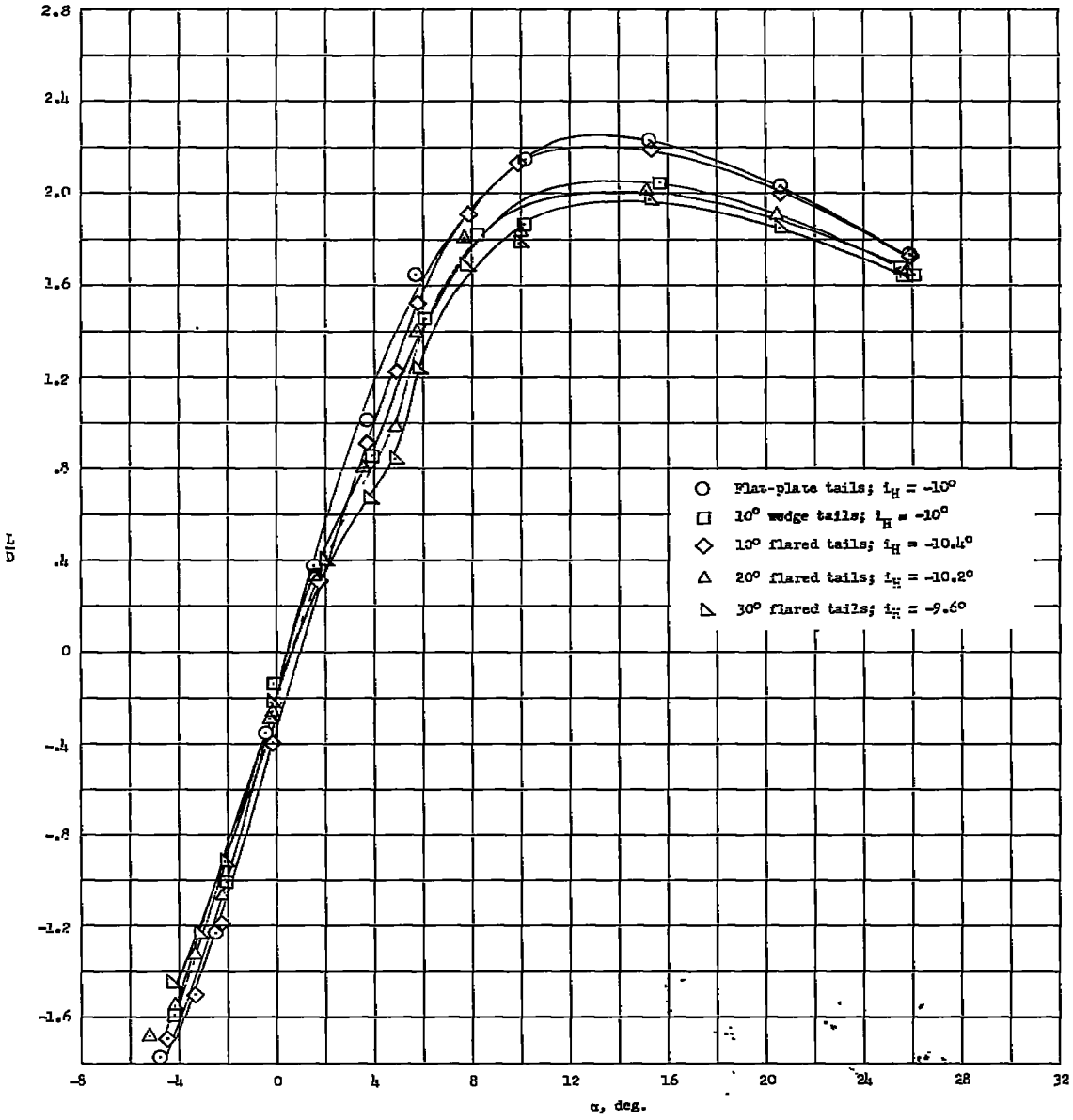

(b) $i_H \approx -10^\circ$; $\beta = 0^\circ$.

Figure 12.- Concluded.

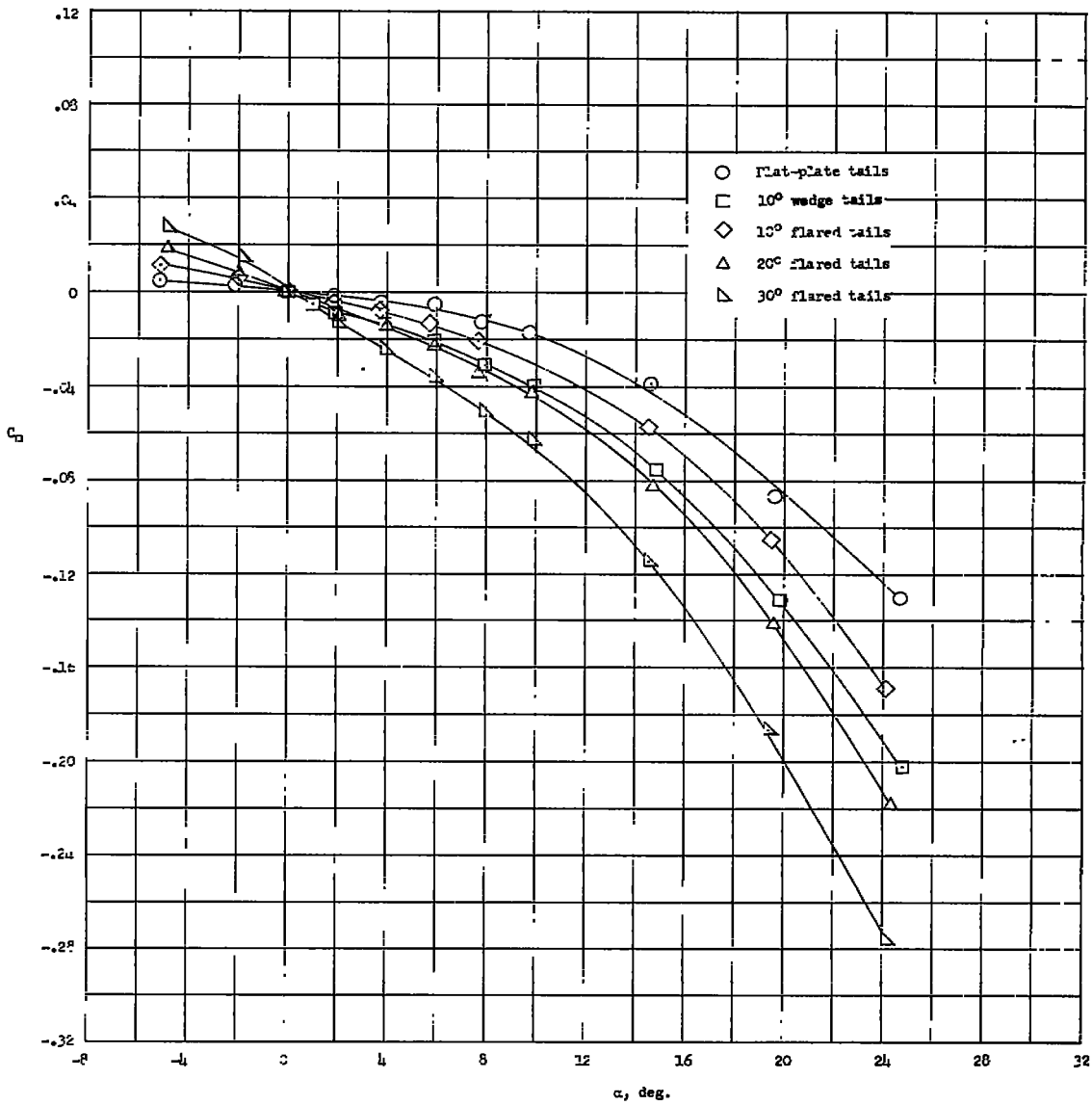

(a) Complete model configuration; $i_H = 0^\circ$; $\beta = 0^\circ$.

Figure 13.- Effect of tail airfoil section on the variation of pitching-moment coefficient with angle of attack for the complete model and body-tail configurations. M = 6.86; R = 343,000; stability-axis data.

[redacted]

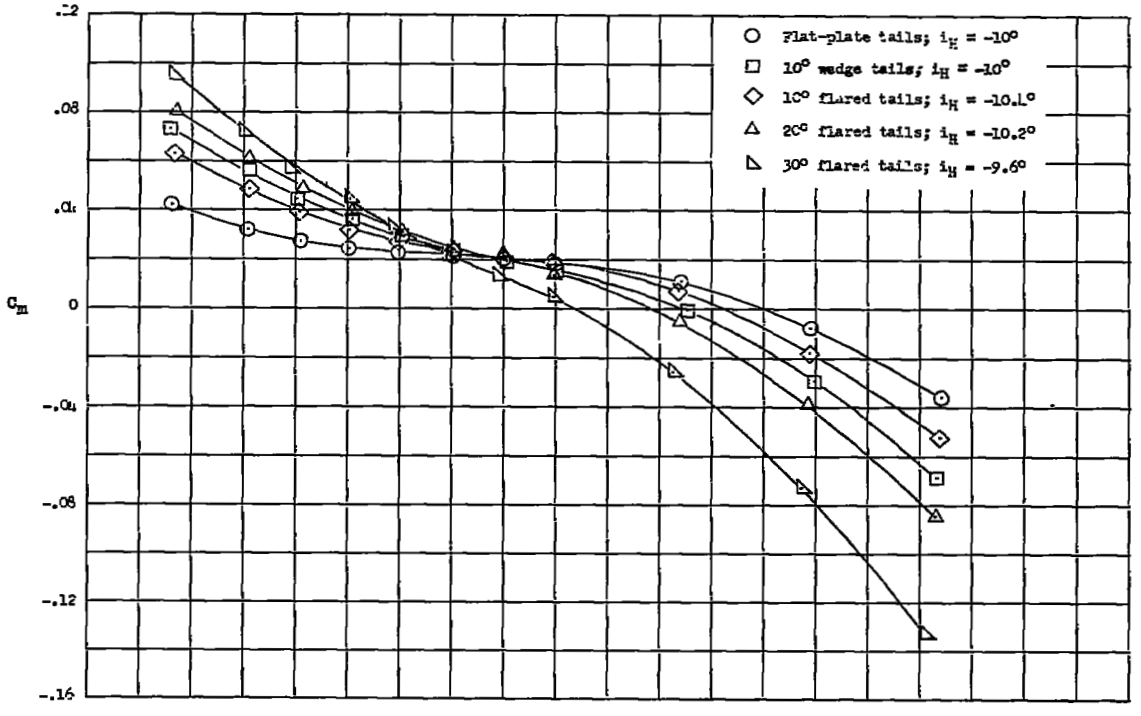

(b) Body-tail configuration; $i_H \approx -10^\circ$; $\beta = 0^\circ$.

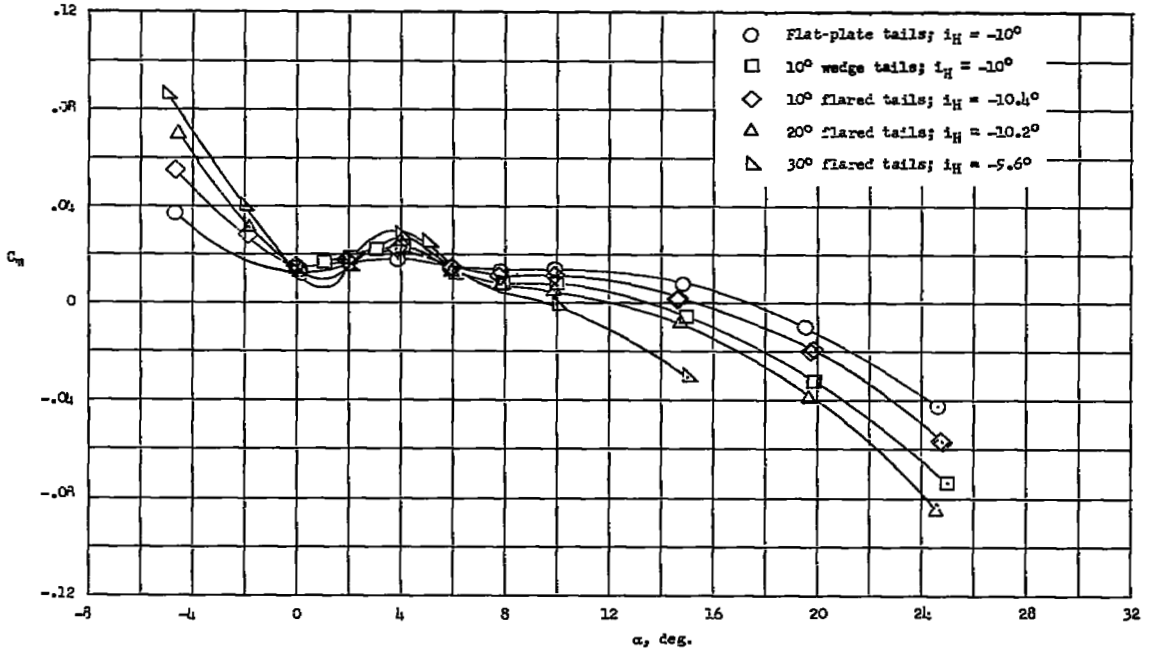

(c) Complete model configuration; $i_H \approx -10^\circ$; $\beta = 0^\circ$.

Figure 13.- Concluded.

[redacted]

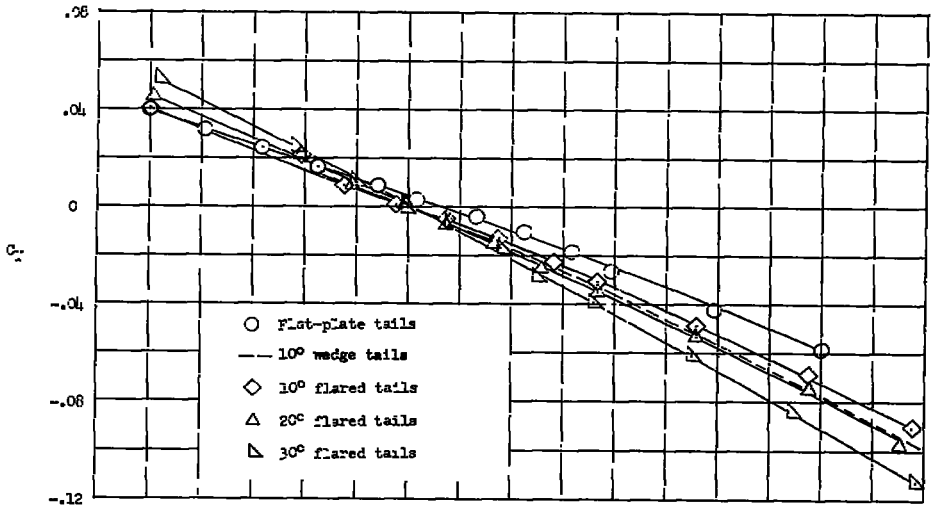

(a) Lateral-force coefficient.

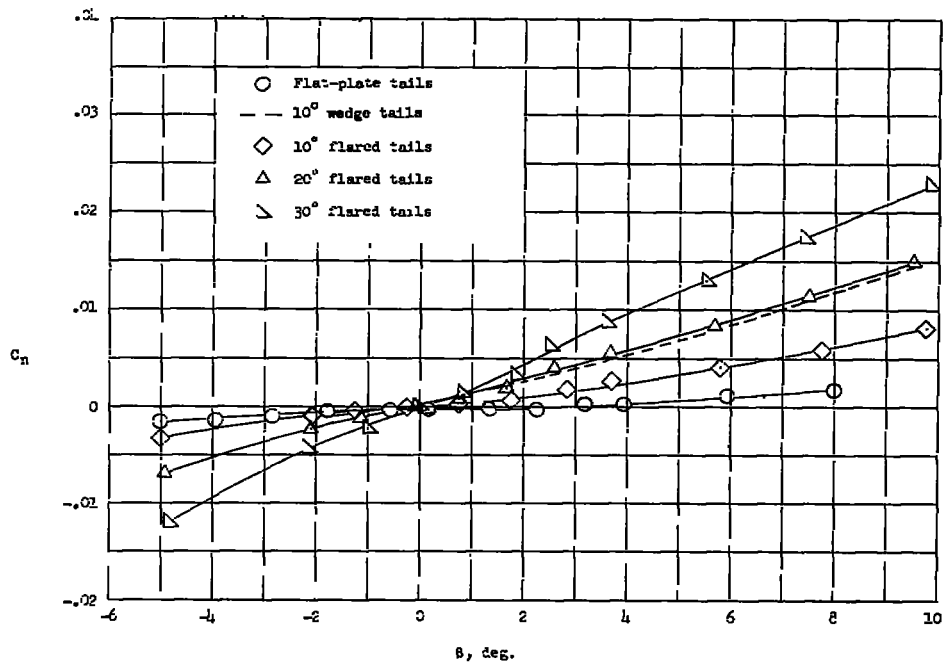

(b) Yawing-moment coefficient.

Figure 14.- Effect of tail airfoil section on the variations of the lateral-force coefficient, yawing-moment coefficient, and rolling-moment coefficient with sideslip angle for the complete model configuration. M = 6.86; R = 343,000; body-axis data; $\alpha = 0^\circ$.

[redacted]

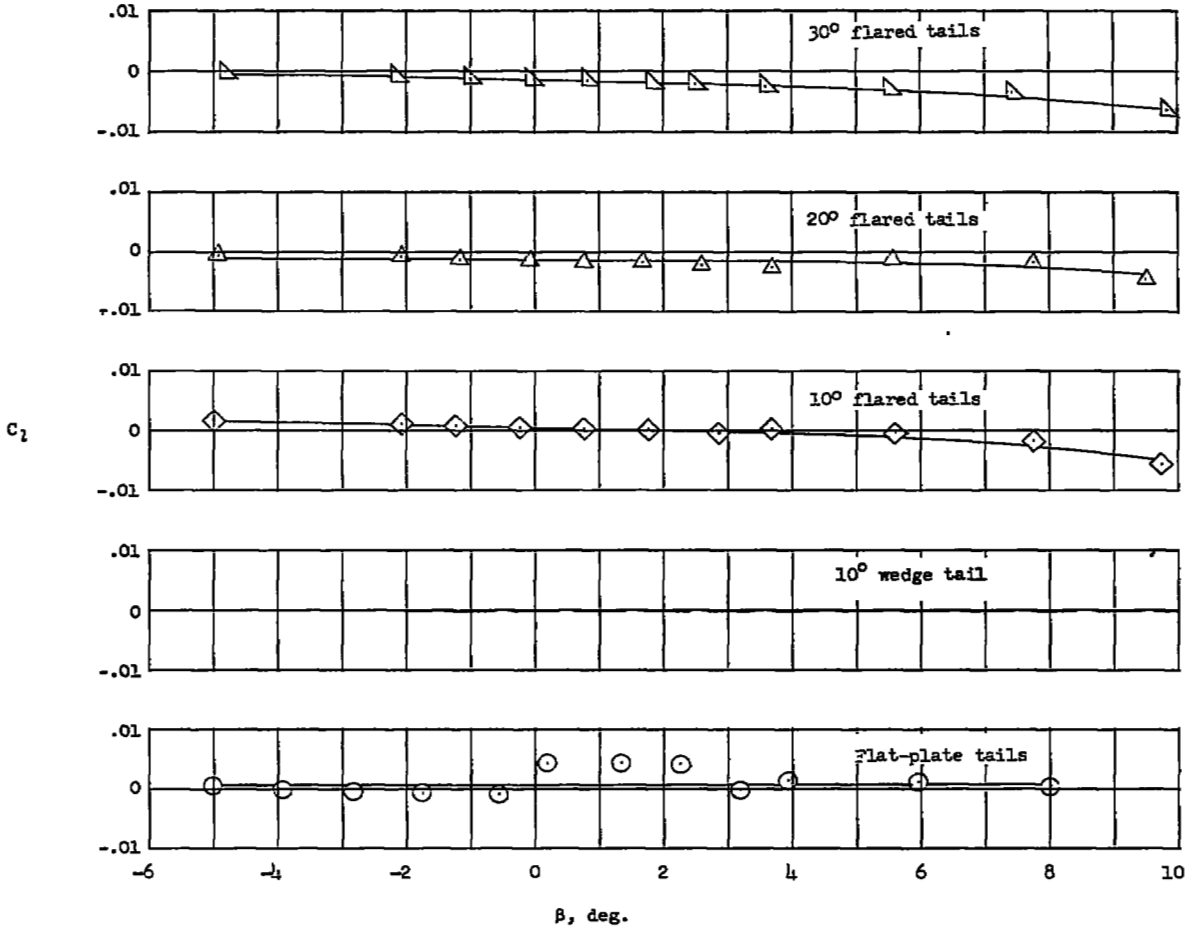

(c) Rolling-moment coefficient.

Figure 14.- Concluded.

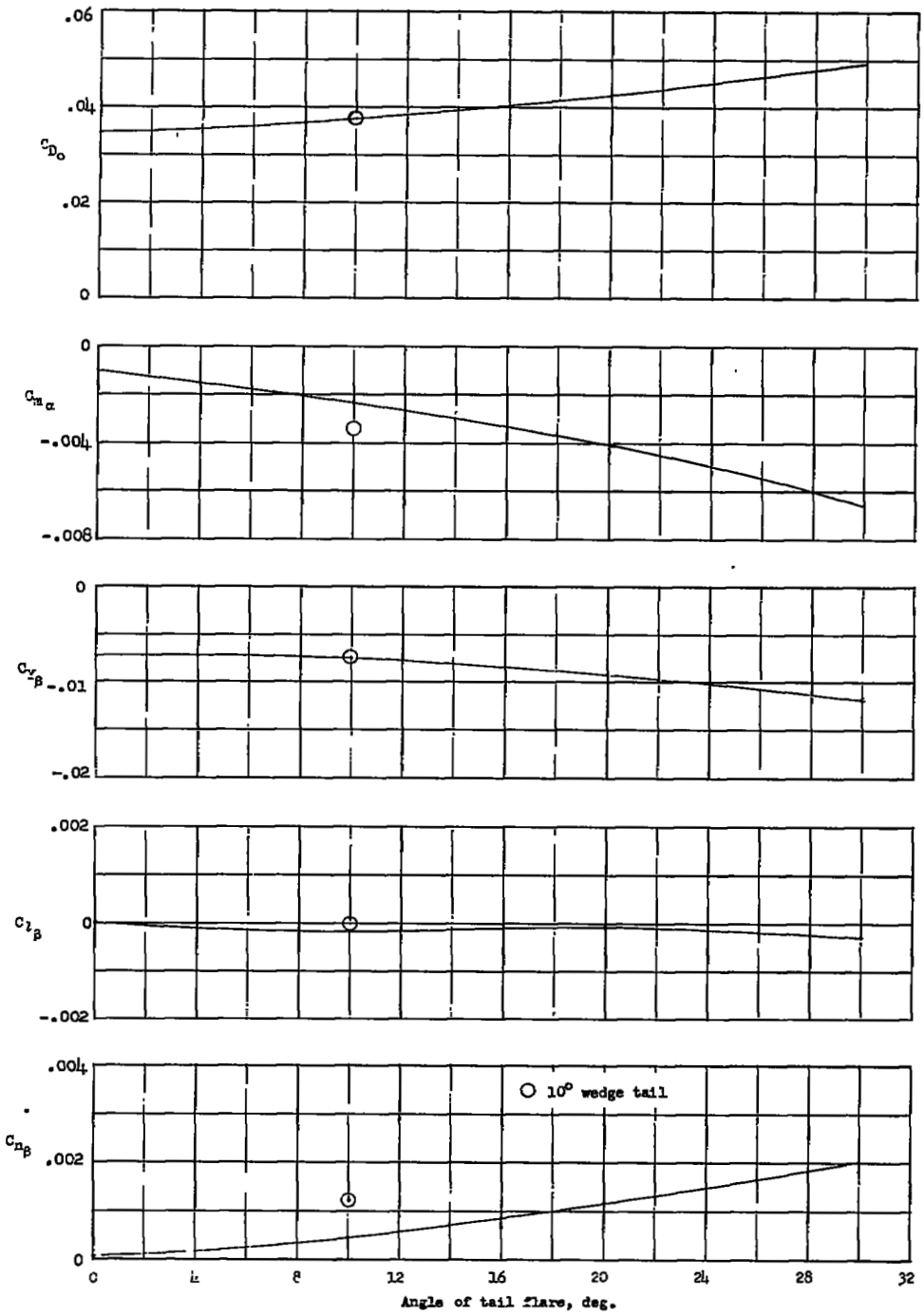

Figure 15.- Summary of the variation of the static stability derivatives and minimum drag coefficient with angle of tail flare for the complete model. $\alpha = 0^{\circ}$; M = 6.86; R = 343,000.

[redacted]

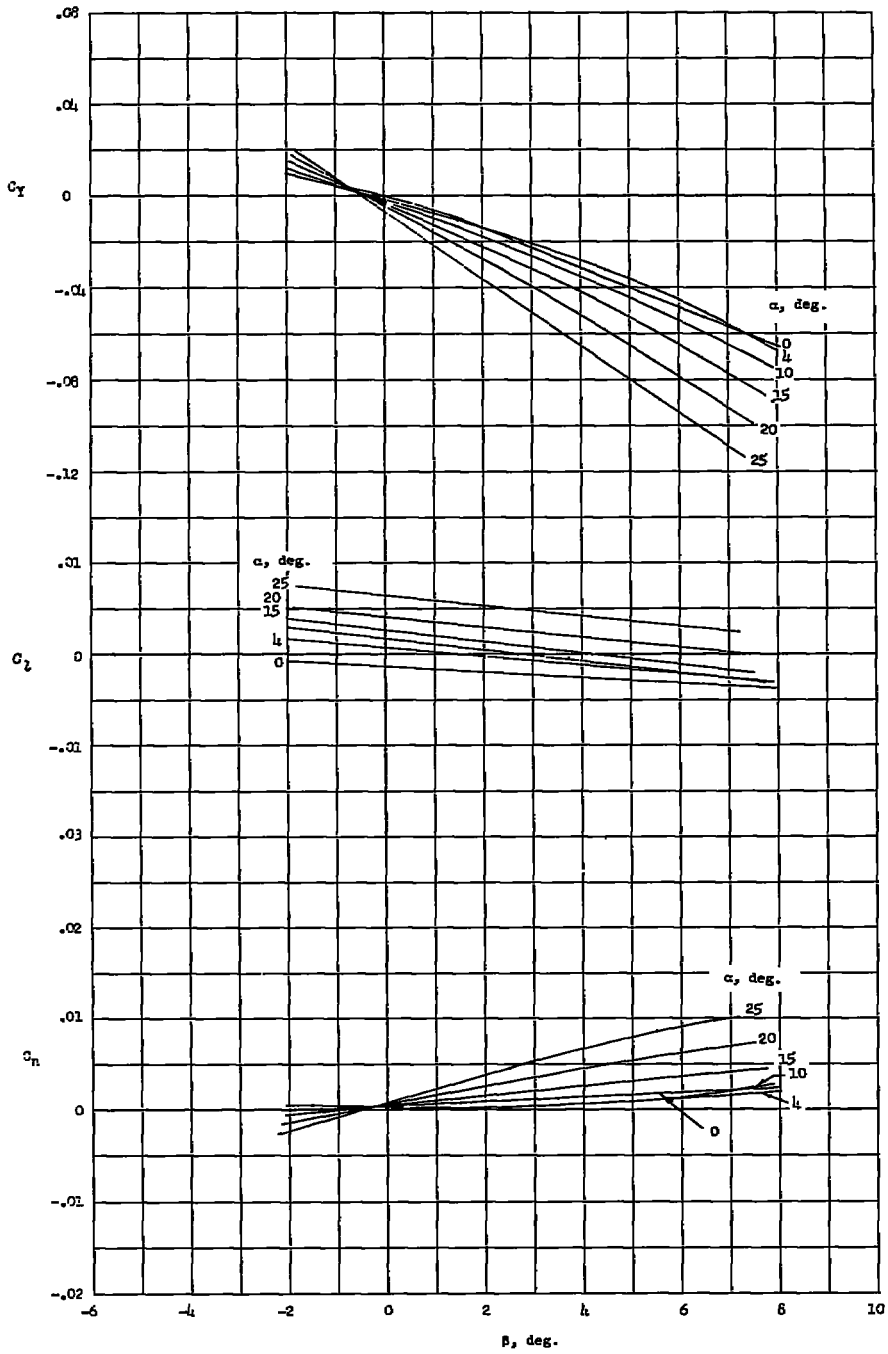

Figure 16.- Variation of the lateral-force coefficient, rolling-moment coefficient, and yawing-moment coefficient with sideslip angle for the complete model using the stub-tail configuration with 10° wedge tail airfoil sections. M = 6.86; R = 343,000; body-axis data.

[redacted]

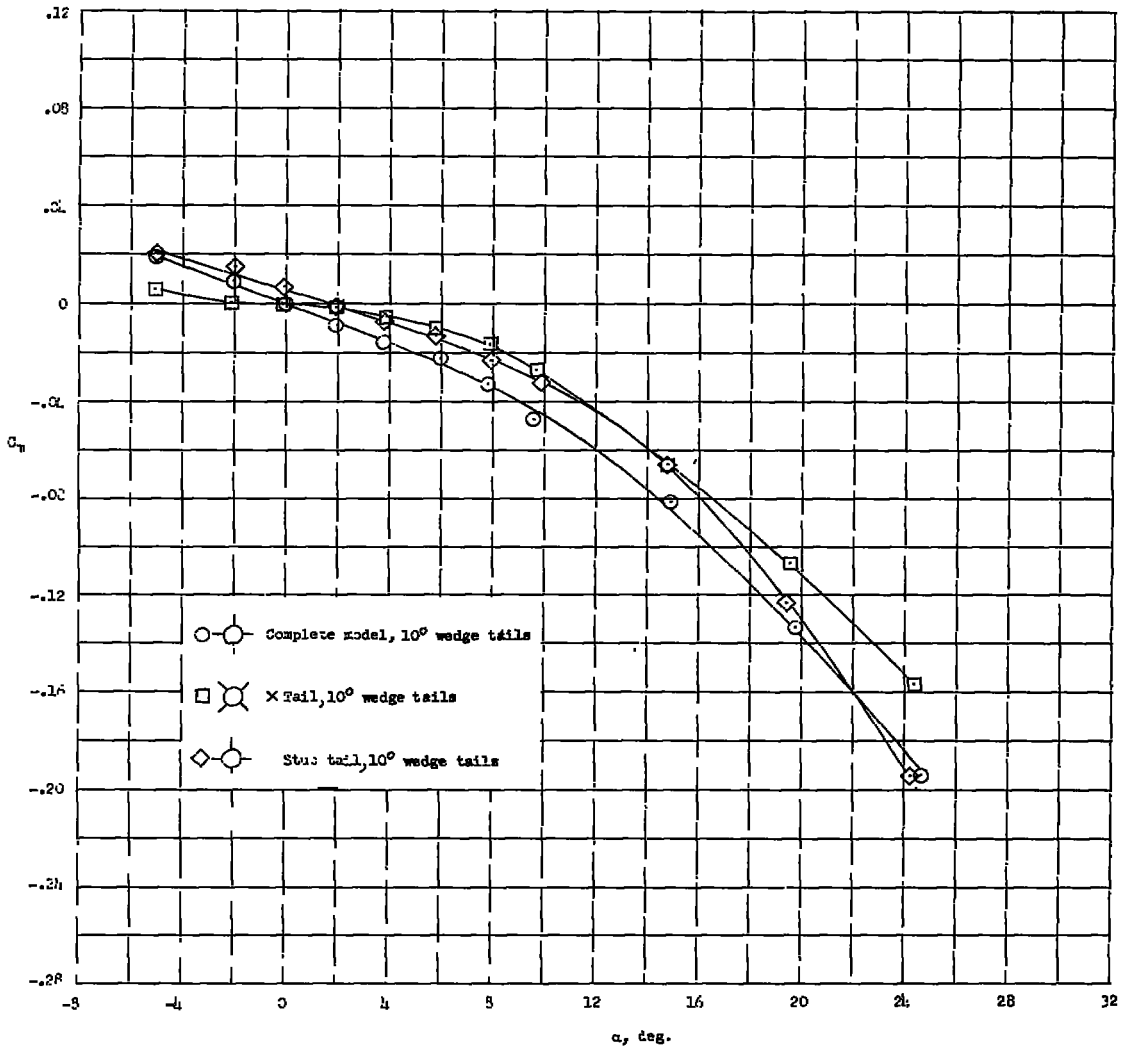

Figure 17.- Effect of tail-surface location and geometry on the variation of pitching-moment coefficient with angle of attack for the complete model configuration with 10° wedge sections. $i_H = 0°$; $\beta = 0°$; M = 6.86; R = 343,000; stability-axis data.

[redacted]

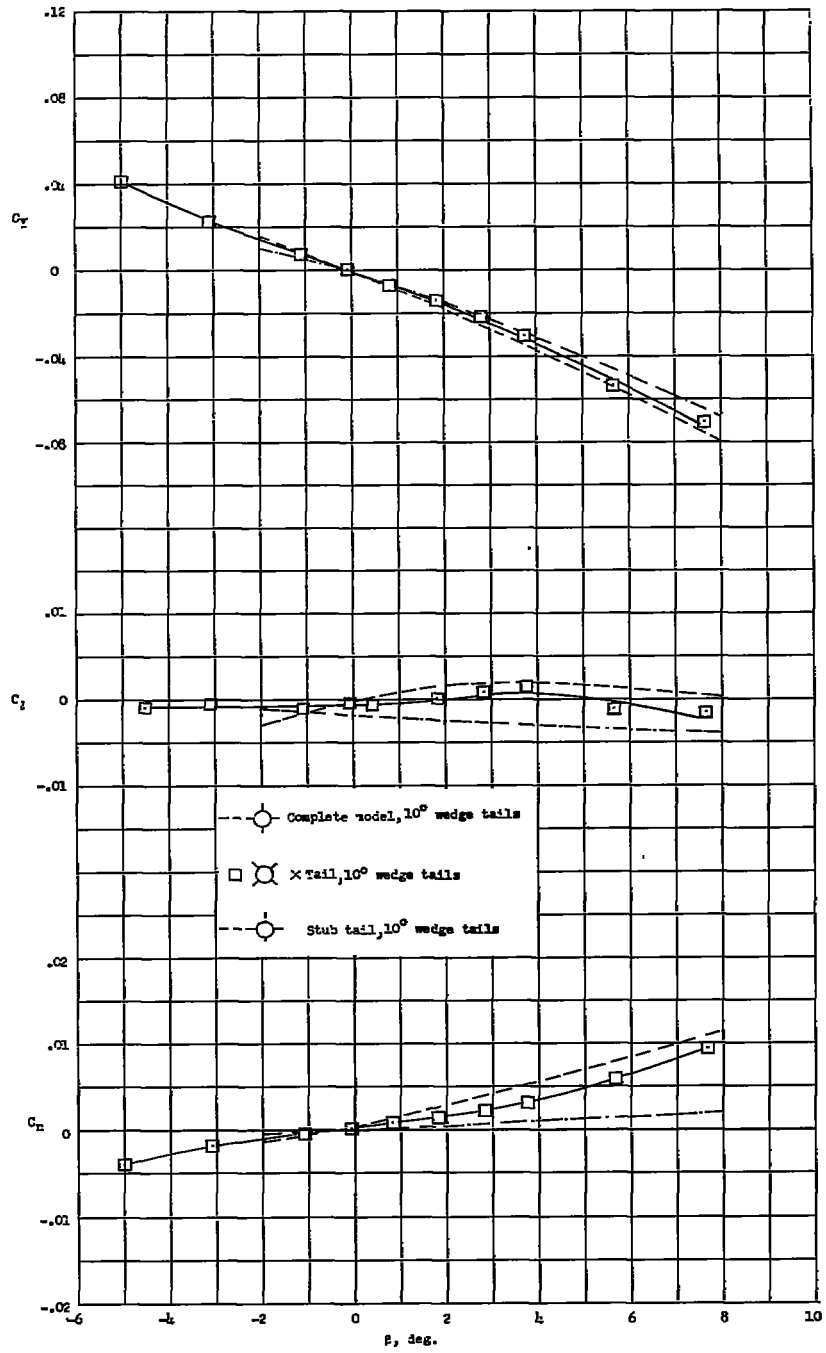

Figure 18.- Effect of tail-surface location and geometry on the variation of lateral-force coefficient, rolling-moment coefficient, and yawing-moment coefficient with sideslip angle for the complete model configuration. M = 6.86; R = 343,000; body-axis data; $\alpha = 0^\circ$.

[redacted]

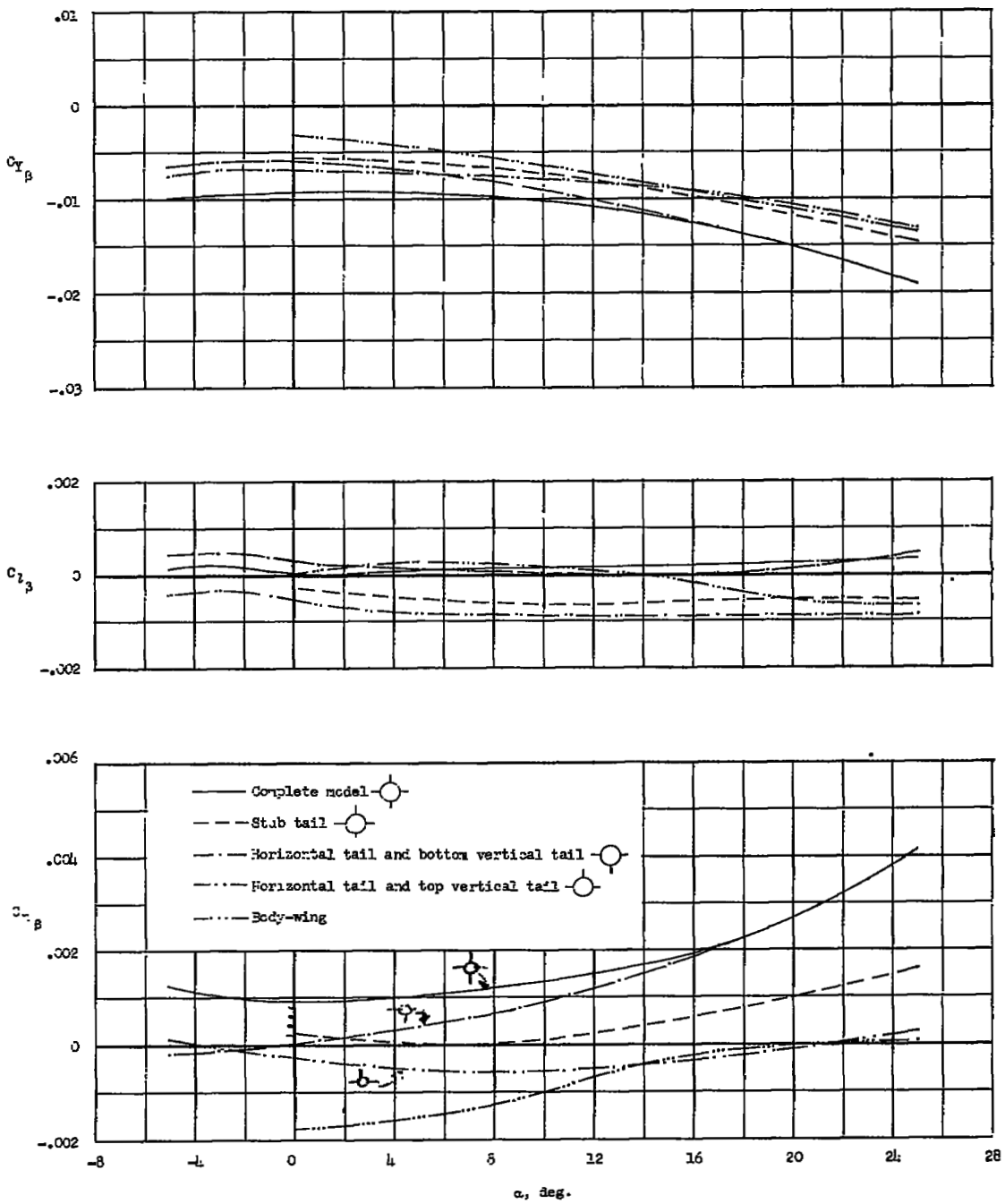

Figure 19.- Variation of the lateral-stability parameters C_{Y_β}, C_{l_β}, and C_{n_β} at $\alpha = 0^\circ$ with angle of attack for the complete model using various tail arrangements with 10° wedge tail airfoil sections. M = 6.86; R = 343,000; body-axis data.

(a) Complete model with flat-plate tails.

(b) Complete model with 10° flared tails.

(c) Complete model with 20° flared tails.

(d) Complete model with 30° flared tails. L-89314

Figure 20.- Typical schlieren photographs of complete model with various tail airfoil sections. M = 6.86; R = 343,000.

[redacted]

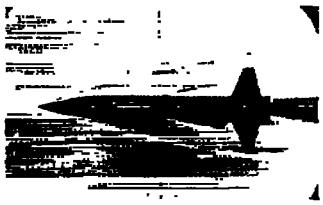

$\alpha = -.02°$

$\alpha = 14.78°$

(a) Complete model with 10° wedge tails.

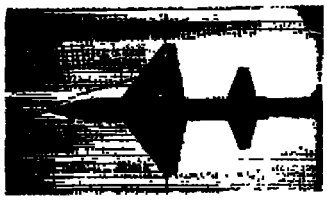

$\alpha = 20°$ $\beta = 0°$

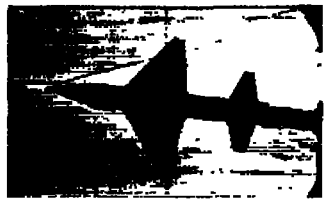

$\alpha = 20°$ $\beta = -8°$

(b) Complete model with 10° wedge tails.

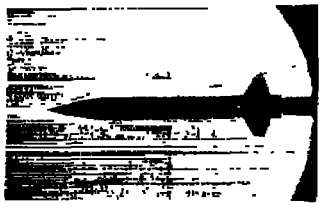

$\alpha = -.17°$

$\alpha = 14.75°$

(c) X-tail configuration.

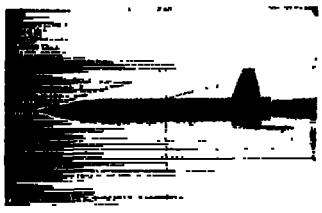

$\alpha = -.08°$

$\alpha = 14.67°$

(d) Stub-tail configuration. L-89315

Figure 21.- Typical schlieren photographs of complete model with various tail arrangements using 10° wedge tail sections. M = 6.86; R = 343,000.